

Chemical composition of A–F type post-AGB candidates

Sunetra Giridhar^{1*}, R. Molina^{2,3}, A. Arellano Ferro⁴ and G. Selvakumar⁵

¹*Indian Institute of Astrophysics, Bangalore 560034, India*

²*Universidad Central de Venezuela*

³*Universidad Nacional Experimental del Táchira, Venezuela*

⁴*Instituto de Astronomía, Universidad Nacional Autónoma de México, Mexico*

⁵*Indian Institute of Astrophysics, Vainu Bappu Observatory, Kavalur, India*

Accepted 2010 March 16. Received 2010 March 15; in original form 2010 January 7

ABSTRACT

An abundance analysis has been conducted for a sample of nine post-AGB candidate stars; eight of them have not been explored before. We find four very promising objects like HD 105262, HD 53300 and CpD–62°5428 among them. We find strong evidence of dust-gas separation through selective depletion of refractive elements in HD 105262. The same effect is also observed in HD 53300, CpD–62°5428 and HD 114855 although abundance peculiarities are relatively smaller for the last two stars. We find strong enrichment of nitrogen for HD 725, HD 842, HD 1457, HD 9233 and HD 61227 but no further evidence to support their post-AGB nature. We have compared the observed [N/C] ratios of these stars with the predictions of evolutionary models which include the rotation induced mixing.

Key words: Post-AGB stars, abundances, circumstellar matter: stars.

1 INTRODUCTION

The post-AGB stars (hereinafter PAGB) are the late stage of evolution of low and intermediate mass stars (1 to $8M_{\odot}$) when they transit from AGB to Planetary Nebulae (PN). Since at the end of AGB evolution, most of the outer envelope is lost, circumstellar shells (detectable in infrared sub-millimeter to radio wavelengths) are commonly observed. However, for less massive progenitors, the longer transition times would result in the dissipation of circumstellar material for them. The atmospheric chemical compositions of PAGB stars and their circumstellar envelopes are those inherited from the local interstellar medium (ISM) but strongly modulated by the products of nucleosynthesis being dredge-up at different stages of evolution through successive mixing events. They enrich ISM with the products of nucleosynthesis through strong stellar winds. They are important contributors of C, N and s-process elements to the ISM. AGB evolution has been described in Herwig (2005) and post-AGB evolution in van Winckel (2003) and García-Lario(2006).

Among intermediate mass stars, those in mass range $2-4M_{\odot}$ would experience Third Dredge Up (TDU) where the the product of helium burning as well as s-process elements are transported to the outer envelope and will become carbon stars ($C/O > 1$). On the other hand, low mass stars

($M < 1.8M_{\odot}$) may not undergo sufficient thermal pulses and subsequent dredge up to reach $C/O > 1$ stage. In higher mass stars the carbon would be quickly converted to nitrogen due to hot bottom burning (HBB) thereby preventing them from becoming carbon stars (Lattanzio et al. 1996, Groenewegen & Marigo 2004, Herwig 2005).

However, the metallicity also has strong influence on the mass limits which determines the chemical dichotomy. The minimum mass needed to activate the HBB, number of thermal pulses needed to produce carbon stars and the efficiency of the dredge up are strongly affected by metallicity. This effect can be seen through the higher proportion of C-rich PN found in the metal-poor systems like Magellanic Clouds.

Although the basic scheme of the post-AGB evolution as presented by Iben & Renzini (1983) is generally accepted, these AGB models and the calculations of yields from AGB were affected by the number of quantities e.g mass-loss, mixing length being kept as free parameters. Further development by Groenewegen & de Jong (1993), Boothroyd & Sackmann (1999) made better approximations for these parameters thereby getting better agreement with observations. But still these models are called synthetic models since they use analytical expression for thermal pulse phase. More complete models by Karakas et al. (2002), Herwig (2004) follow all the pulses in detail. A careful testing of these model prediction is warranted since the yield they produce still depends upon the adopted treatment of convection and mass-loss.

* E-mail: giridhar@iiap.res.in (SG); rmolina@unet.edu.ve (RM); armando@astroscu.unam.mx (AAF); selva@iiap.res.in (GS)

1.1 Post-AGB detections

Observationally, a range of objects with diverse characteristics are found under this class, hence different strategies to identify them.

The IRAS two color diagrams have been very useful in detecting these objects (Kwok et al. 1987, van der Veen et al. 1988; 1989, Van de Steene & Pottasch 1993, García-Lario et al. 1997, Van de Steene et al. 2000 and more recently Suárez et al. 2006). These authors have studied candidates with PN like colors with supplementary data in longer wavelengths to confirm their advanced evolutionary status. These objects were found to be very faint in optical wavelengths.

The investigation of optically bright IRAS sources with IR fluxes pointing to the existence of dusty shells (see e.g. Hrivnak et al. 1989, Pottasch & Parthasarathy 1988, Oudmaijer et al. 1992, van Winckel 1997) has also led to the detection of many post-AGB stars. However, these stars occupy different parts of the IRAS two color diagram.

The systematic studies of high galactic latitude supergiants e.g. by Luck, Lambert & Bond 1990 from the candidate list of Bidelman (1951) have also resulted in more detections. Although many display double-peaked energy distributions, objects like HR 6144 and BD+39°4926 are exceptions. Among these high galactic latitude supergiants, a small subgroup called UU Her characterized by high radial velocities small amplitude pulsation and large IR excess also contains sizeable fraction of post-AGB stars.

Hot post-AGB stars are found from the studies of B stars found in the Galactic Halo (McCausland et al. 1992, Conlon et al. 1993, Moehler & Heber 1998). UV bright objects in globular clusters also contain objects like Bernard 29 in M13 (Conlon, Dufton & Keenan 1994), No 1412 in M4 (Brown, Wallerstein & Oke 1990) which show chemical compositions similar to those of halo B stars.

The variable stars like RV Tau and population II Cepheids contain a noticeable fraction of post-AGB stars (Giridhar et al. 1994, Maas et al. 2002, Giridhar et al. 2005, Maas, Giridhar & Lambert 2007). It is a consequence of post-AGB evolutionary track intersecting the high luminosity end of instability strip.

The above mentioned detections were made on samples strongly biased towards candidates showing optically brighter counterparts, generally stars located at high galactic latitude and belonging to low mass populations. More recent color selected and flux limited samples have led to the detection of rapidly evolving heavily obscured post-AGB stars. These objects included in GLMP catalog (García-Lario 1992) do not show preference to F and G spectral type and high galactic latitude but have flatter distribution in spectral type and follow galactic distribution which corresponds to more massive population (García-Lario 2006). The center stars of these highly obscured post-AGB stars is usually of B type suggesting a fast post-AGB evolution. They possess circumstellar molecular shells which are detectable in CO or OH at sub-millimeter or radio wavelengths. Most of these objects are O-rich which is expected for stars developing the HBB at the AGB phase.

1.2 The observed chemical compositions

The chemical composition studies indicate a diverse behaviour too. The classical post-AGB stars (displaying double peaked SED) with enhancement of carbon (carbon - rich) and s-process elements caused by Third Dredge-Up make only a relatively smaller fraction of the known post-AGB stars. The well-known examples are HD 56126, IRAS 065330-0213, HD 158616, HD 187785 (Klochkova 1995, Bakker & Lambert 1998, Reyniers 2002 and Reddy et al. 2002). Their IR spectrum contains 21 micron features.

The other subgroup (O-rich) also show double peaked SED but have no signature of TDU. The typical examples are HD 161796, 89 Her, HD 133656, SAO 239853, HR 4912 (Luck, Lambert & Bond 1983, van Winckel 1997, Giridhar, Arellano Ferro & Parrao 1997).

A subgroup with C/O nearly one but showing selective depletion of easily condensable elements like Fe, Cr, Ca and Sc has been identified. HR 4049, HD 46703, BD+39°4926, HD 52961 (Lambert, Hinkle & Luck 1988, Bond & Luck 1987, Waelkens et al. 1991) are well known post-AGB stars showing this effect. The same effect is also seen in RV Tau stars; e.g. IW Car, AC Her, EP Lyr, AD Aql and many others (Giridhar et al. 1994, Giridhar, Lambert & Gonzalez 2000, Giridhar et al. 2005, Maas, van Winckel & Waelkens 2002, van Winckel et al. 1998, Gonzalez et al. 1997) and also in population II Cepheids like ST Pup, CC Lyr (Gonzalez & Wallerstein 1996, Maas et al. 2007). Scenarios based upon a single star with dust-gas separation occurring in the stellar wind and binary stars with dust-gas separation occurring into circumbinary disks have been discussed in several papers. Keplerian circumbinary disk has been observed for HD 44179 van Winckel et al. (1995), Waters et al. (1998) and more recently by Bujarrabal et al. (2005). More such detection of circumbinary disks by de Ruyter et al. (2006), van Winckel (2007) and interferometric studies by Derroo et al. (2006; 2007) have lent support to the existence of compact passive disc around many post-AGB binaries.

A mixed chemistry has been observed in the infrared spectra of some evolved objects where features of both O-rich and C-rich dust species are present e.g. J-type carbon stars exhibiting silicate dust emission (Lloyd Evans 1990), PAGB HD 44179 showing O-rich circumbinary disk (van Winckel et al. 1995, Waters et al. 1998) and EP Lyr shows emission features of C-PAH emission as well as those of crystalline silicates Gielen et al. (2009).

The analysis of 350 ISO spectra of post-AGB and PN by García-Lario & Perea Calderón (2003) has made a strong impact on our understanding of PAGB - PN transition based upon the shape of the infrared spectrum and evolution of gas phase molecular bands and that of the solid state features detected in the 1 to 60 μ spectral range. These authors have identified two main chemical evolutionary sequences (for C-rich and O-rich stars) through which the process of condensation and growth of the dust-grain produced in circumstellar envelopes till the star becomes PN can be followed.

Given the importance of post-AGB objects in understanding the late stages of evolution of low and intermediate mass stars and their contribution to enrichment of the interstellar medium (ISM), it is hardly surprising that the detection of new post-AGB stars still continue to be one of the most important scientific objectives of many surveys.

The recent Torun catalog of post-AGB objects (Szczerba et al. 2007) contains 326 likely post-AGB stars and 107 possible candidates.

We continue our exploration of optically bright post-AGB candidates, based upon the criteria of their PN like colors in two color diagrams of van der Veen & Habing (1988), high-galactic latitude and also Strömberg c_1 index (as listed in Bidelman 1993) with modest facilities available. Our sustained effort in the past has been rewarded with the detection of many interesting objects such as HD 725, HD 27381, HD 137569, HD 172481, HD 21853 and HD 331319 (Arellano Ferro, Giridhar & Mathias 2001 and Giridhar & Arellano Ferro 2005). This paper is the third in a series devoted to the search of more post-AGB stars among high-galactic latitude A-G supergiants (see Table 1).

In section 2 we present description of the observational material used and reduction technique. The abundance analysis approach and error analysis is presented in section 3. The results of individual stars are presented in section 4. In section 5 we discuss large nitrogen enhancements observed in some sample stars. Section 6 contains the summary and conclusions.

2 OBSERVATIONS AND DATA REDUCTIONS

The spectra for this work were obtained largely using the ELODIE spectrograph at 1.93m telescope of the Haute-Provence Observatory (OHP) giving 42,000 resolution (Baranne et al. 1996) and the echelle spectrometer at 2.3m telescope of the Vainu Bappu Observatory (VBO), Kavalur giving 28,000 resolution in the slitless mode (Kameswara Rao et al. 2005). A few, but very important spectra were also obtained with MIKE spectrograph on the 6.5m Magellan telescope at the Las Campanas Observatory giving about 24,000 resolution and a spectral coverage from 3350 to 9400 Å, and the 2D Coudé echelle spectrograph (Tull et al. 1995) on the 2.7m telescope at the McDonald Observatory giving 60,000 resolution.

The spectroscopic reductions were carried out using the tasks contained in IRAF software of NOAO. Our program stars were generally in the temperature range 7000K to 7500K hence the spectra were not crowded enabling us to measure the line strengths with an accuracy of 8 to 10% at the resolution employed.

3 ABUNDANCE ANALYSIS

We have used LTE model atmosphere grid of Castelli & Kurucz (2003). The spectrum synthesis code SPECTRUM of R.O. Gray and the 2002 version of MOOG written by C. Sneden were used. The assumptions are standard, LTE, plane parallel atmosphere, hydrostatic equilibrium and flux conservation. As explained in Giridhar & Arellano Ferro (2005), the 2002 version of MOOG was not found suitable for the abundances of light elements such as CNO for stars hotter than G type. The problem was found to be aggravating with increasing temperatures. We have used MOOG for estimating the atmospheric parameters and the abundances of the Fe-peak elements. These results were confirmed with SPECTRUM code and the CNO abundances were derived using

this code. The hydrogen lines for a few stars were affected by emission components.

The microturbulence velocity (ξ) is derived by requiring that the derived abundances are independent of line strengths. We have used Fe II lines instead of Fe I lines since appreciable departure from local thermodynamic equilibrium (LTE) are known to occur for Fe I lines (Boyarchuck et al. 1985, Thévenin & Idiart 1999). It was shown by Schiller & Przybilla (2008) that Fe II lines are not seriously affected by departure from LTE and ξ is independent of depth in the atmosphere.

For temperature determinations, the photometric estimates were used as initial guess and refined by requiring that derived abundances are independent of low excitation potential (LEP) of the lines. The gravity can be derived by requiring the Fe I and Fe II giving the same abundance. However, this provides a locus in ($T_{\text{eff}}, \log g$) plane. Additional loci can be obtained by fitting the Balmer line profiles and ionization equilibrium of Mg I/Mg II, Si I/Si II, Sc I/Sc II, Ti I/Ti II and Cr I/Cr II. The intersection of these loci gives good estimate of temperatures and gravities. However, for some stars the hydrogen lines were affected by emission components so that criteria could not be used.

Within the accuracies of measured equivalent widths, the microturbulence velocity could be estimated with an accuracy of $\pm 0.5 \text{ km s}^{-1}$, temperature with $\pm 200 \text{ K}$ and $\log g$ of 0.25 cm s^{-2} .

The derived atmospheric parameters and radial velocities for the program stars are presented in Table 2.

The sensitivity of the derived abundances to the uncertainties of atmospheric parameters T_{eff} , $\log g$, and ξ are summarized in Table 3. For three stars representing the temperature range of our sample, we present changes in abundances caused by varying atmospheric parameter by 200K, 0.25 cm s^{-2} and 0.5 km s^{-1} with respect to the chosen model for each star.

The total error is evaluated by taking the square root of the sum of the square of individual errors associated with uncertainties in temperatures and gravities. The error bars in the abundance plots correspond to this total error.

3.1 Sources of $\log gf$ values

We have used the compilation of Führt & Wiese (2006) for Fe I and Fe II lines. Experimental $\log gf$ values of high accuracy (5 to 10 %) are available for a large fraction of iron lines. For Fe II lines $\log gf$ values of Melendez & Barbuy (2009) were used when available. For Cr I, most recent gf values of Sobek et al. (2007) are employed which have accuracies between 10 to 25%. For light elements C,N,O we have used lines available in NIST data base in category B to C which implies that gf values are accurate within 10-25%. For Na and Mg the accuracies of gf values are 10 to 15%. For light elements as well as for Fe-peak elements the gf values given in NIST data base were used. For Y II gf values of Hannaford et al. (1982), Zr II Biemont et al. (1981) and Ljung et al. (2006) were used. For Ba II, gf values of Gallagher (1967) and Davidson et al. (1992) were used. For La II Lawler et al. (2001a), Ce II Lawler et al. (2009), Eu II La II Lawler et al. (2001b), for Sm II Lawler et al. 2006, for Nd II Hartog et al. (2003), for Pr II, Dy II Sneden et al. (2009) were used. These recent determinations of $\log gf$

Table 1. Basic data for sample stars.

Star	SpT.	V (mag.)	l ($^{\circ}$)	b ($^{\circ}$)	IRAS	12 μ (Jy)	25 μ (Jy)	60 μ (Jy)	100 μ (Jy)
HD 725	F5Ib-II	7.08	117.56	-5.1	00091+5659	0.36	0.25L	0.40L	14.43L
HD 842	A9Iab	7.96	117.52	-6.6					
HD 1457	F0Iab	7.85	118.92	-2.2					
HD 9233	A4Iab	8.10	128.15	-3.3	01289+5853	0.31	0.37L	0.40L	9.27L
HD 53300	A0Ib	7.00	219.12	+0.4	07018-0513	0.75	0.31	0.41:	2.80:
HD 61227	F0Ib	6.38	239.15	-1.2	07351-2339	0.62	0.25L	0.40L	6.36L
HD 105262	B9 Ib	7.09	264.5	+72.4					
HD 114855	F5Ia/Iab	8.39	306.24	+8.0	13110-5425	0.31L	2.11	7.60	5.33
CpD -62 $^{\circ}$ 5428	A7Iab	9.94	326.20	-11.1	16399-6247	0.25L	1.28	1.94	2.17L

Table 2. Derived physical parameters and radial velocities for program stars.

Star	T_{eff} (K)	log g	ξ (km s $^{-1}$)	[Fe/H]	$V_r(\text{Hel})$ (km s $^{-1}$)	Observatory	Date Obs.
HD 725	7000	1.0	4.65	-0.20	-56.9	OHP	1999 Jul 6
					-58.9	VBO	2006 Dec 8
HD 842	7000	1.0	2.3	-0.25	-31.2	OHP	2000 Oct 7
					-30.4	VBO	2008 Sep 22
HD 1457	7300	0.75	3.4	-0.20	-38.5	OHP	2000 Oct 10
					-38.2	VBO	2008 Oct 9
HD 9233	7750	1.0	4.2	-0.21	-29.9	OHP	1999 Jul 11
					-31.9	VBO	2008 Sep 22
HD 53300	7500	0.5	2.4	-0.62	+58.4	McD	2007 Nov 2
					+58.3	VBO	2006 Feb 18
HD 61227	7000	1.0	4.0	-0.38	+18.5	OHP	2000 Oct 7
					+18.3	VBO	2005 Jan 22
					+17.9	VBO	2005 Mar 28
					+18.4	VBO	2006 Feb 10
					+18.2	VBO	2006 Feb 14
					+18.0	VBO	2006 Feb 18
HD 105262	8500	1.5	2.8	-1.87	+18.5	McD	2009 May 19
HD 114855	6000	0.5	4.7	-0.11	+73.0	LCO	2008 Feb 14
					-3.3	VBO	2006 Feb 16
					-2.6	VBO	2006 Feb 17
					-13.6	VBO	2009 Jan 2
CpD -62 $^{\circ}$ 5428	7250	0.5	4.6	-0.45	+2.5	VBO	2009 Jul 11
					-29.9	LCO	2008 Feb 14

Sources of spectra: Haute Provence Observatory (OHP), Vainu Bappu Observatory (VBO), Las Campanas Observatory (LCO), McDonald Observatory (McD).

values for heavy elements based upon accurate estimates of radiative lifetimes and branching fractions are believed to have accuracies of 10%.

3.2 Errors caused by NLTE effects

The carbon abundance is derived using lines in 4770-75 \AA , 5380 \AA and 7110-15 \AA regions. Venn (1995) has determined CNO abundances for a sample of 22 A type supergiants and has calculated NLTE corrections. The lines used in the analysis have additional lines around 9100 \AA but the corrections are available for the important lines near 7110 \AA used in the present work (Table 6 and Fig. 6 of Venn 1995). The NLTE corrections are temperature dependent, becoming large at higher temperature and also vary from multiplet to multiplet. For example, the correction may vary between -0.1

to -0.5 dex for the temperature range of 7400K to 9950K for the C I lines at 7110-20 \AA region. For NI the lines in 7420-70 \AA , 8160-80 \AA , 8710-40 \AA were generally employed. A similar temperature dependent NLTE correction is found by Venn (1995) for NI lines of different multiplets. Here the correction may vary between -0.3 to -1.0 dex for the above mentioned temperature range (Table 8 of Venn 1995). Takeda & Takada-Hidai (1998) have calculated NLTE correction for oxygen abundance using OI lines at 6155-6160 \AA region. For the above mentioned temperatures range the correction varies from -0.1 to -0.4 dex. The accuracies of NLTE corrections are about ± 0.1 dex.

Table 3. Sensitivity of abundances to the uncertainties in the model parameters for three ranges of temperature.

Specie	ΔT_{eff}	$\Delta \log g$	$\Delta \xi$	ΔT_{eff}	$\Delta \log g$	$\Delta \xi$	ΔT_{eff}	$\Delta \log g$	$\Delta \xi$
	–200K	+0.25	+0.5	–200K	+0.25	+0.5	–200K	+0.25	+0.5
	HD 114855	(6000K)		HD 53300	(7500K)		HD 105262	(8500K)	
C I	+0.05	+0.05	–0.02	–0.18	–0.10	–0.01			
N I	+0.14	+0.07	–0.02	+0.01	+0.01	–0.09	–0.04	+0.00	–0.01
O I	+0.02	+0.02	–0.02	+0.00	+0.01	–0.02	–0.02	+0.00	–0.01
Na I	–0.11	–0.03	–0.01	–0.22	–0.12	–0.01	–0.23	–0.13	+0.00
Mg I	–0.12	–0.04	–0.05	–0.25	–0.13	–0.09	–0.28	–0.14	–0.01
Al I				–0.36	–0.13	–0.13			
Si I	–0.10	–0.03	–0.02	–0.22	–0.12	–0.01	–0.29	–0.14	–0.01
Si II				+0.02	+0.03	–0.22	+0.03	+0.08	–0.04
S I	–0.02	+0.02	–0.01	–0.21	–0.12	–0.01	–0.28	+0.24	+0.00
Ca I	–0.14	–0.03	–0.03	–0.34	–0.18	+0.00			
Ca II				–0.14	–0.06	–0.01	–0.44	–0.24	+0.00
Sc II	–0.09	+0.07	–0.02	–0.18	–0.01	–0.04	–0.23	–0.04	–0.01
Ti II	–0.09	+0.07	–0.04	–0.20	+0.01	–0.03	–0.22	–0.01	–0.02
V I	–0.26	–0.03	–0.01						
V II	–0.09	+0.07	–0.01	–0.17	+0.01	–0.04			
Cr I	–0.22	+0.03	–0.04						
Cr II	–0.03	+0.06	–0.07	–0.13	+0.02	–0.06	–0.12	+0.03	–0.01
Mn I	–0.18	–0.03	–0.03	–0.32	–0.13	–0.01			
Fe I	–0.19	–0.03	–0.03	–0.33	–0.13	–0.02	–0.38	–0.14	+0.01
Fe II	–0.03	+0.06	–0.05	–0.12	+0.02	–0.10	–0.11	+0.04	–0.02
Co I	–0.25	–0.04	–0.01						
Co II	–0.09	+0.05	–0.02						
Ni I	–0.20	–0.03	–0.03	–0.32	–0.13	–0.01			
Cu I	–0.22	–0.03	–0.03						
Zn I	–0.20	–0.03	–0.05	–0.33	–0.15	+0.00			
Sr II				–0.43	–0.10	–0.21			
Y II	–0.14	+0.06	–0.06	–0.30	–0.04	–0.02			
Zr II	–0.18	+0.04	–0.02	–0.22	–0.02	–0.02			
Ba II				–0.49	–0.19	–0.02	–0.32	–0.12	+0.00
La II	–0.15	+0.06	–0.02						
Ce II	–0.16	–0.06	–0.02						
Nd II	–0.20	–0.06	–0.02						
Sm II	–0.16	–0.07	–0.01						

4 ELEMENTAL ABUNDANCES FOR THE SAMPLE STARS

4.1 HD 842

This high galactic latitude A9 supergiants does not have IRAS fluxes although from 2MASS the infrared fluxes in J, H, K have been measured. The Strömgren photometry by Hauck & Mermilliod (1998) and Olsen(1983) in combination with our unpublished empirical calibrations of the reddening-free indices $[m_1]$, $[c_1]$ and $H\beta$, has been employed to estimate T_{eff} in 6800–7200K range. The above empirical calibrations were calculated using 41 stars with spectral types A0 to K0 and luminosity classes I or II. The effective temperatures of the calibrating stars were determined from 13-color photometry (Bravo-Alfaro et al. 1997). The spectral type of A9 and luminosity class I were reiterated by Giridhar & Goswami (2002) who used the strength of Hydrogen lines, Ca II H & K, Ca I 4226 and Mg I feature at 5172–83Å to estimate spectral type, luminosity class for a large sample of standard stars as well as metal-poor stars using the medium resolution spectra.

From the loci of $H\delta$, Fe I/Fe II and Cr I/Cr II we have

estimated a temperature of 7000 ± 250 K and $\log g = 1.0 \pm 0.25$ (Fig. 1).

The radial velocity of -31.1 km s^{-1} has been reported by Gontcharov (2006) and -29.3 km s^{-1} by Grenier et al.(1999). From our OHP spectrum taken on Oct 7, 2000 a radial velocity of $-31.2 \pm 0.3 \text{ km s}^{-1}$ and VBO spectrum taken on Sept 22, 2008 a radial velocity of $-30.4 \pm 0.3 \text{ km s}^{-1}$ is measured. Hence we do not see significant radial velocity variations for this star.

We have done two independent abundance analyses of this star using i) OHP spectrum taken on Oct 7, 2000 and ii) VBO spectrum taken on Sept 22, 2008. The later has lower resolution but more extended coverage in red enabling the CNO analysis.

We have plotted in Fig. 2 the equivalent widths of lines common between OHP and VBO spectra to study the possible systematic effects caused by differences in resolution. In the weak line regime, we notice only small systematic differences between the two sets of equivalent widths. The weak lines are less sensitive to atmospheric parameter variations but are sensitive to resolution. For the spectral type of A-F the spectra being less crowded, the VBO resolution of 28,000 was adequate and enabled us to measure a

Table 4. Elemental abundances for HD 842.

Specie	$\log\epsilon(X)_{\odot}$	OHP (Oct 7 2000) (7000,1.0,2.3)			VBO (Sep 22 2008) (7000,1.0,3.1)			Average	
		[X/H]	N	[X/Fe]	[X/H]	N	[X/Fe]	[X/H]	[X/Fe]
C I	8.39	-0.36 ± 0.11	4	-0.09	-0.27 ± 0.09	11	-0.05	-0.32	-0.07
N I	7.78				$+0.81 \pm 0.09$	syn	+1.03	+0.81	+1.03
O I	8.66	-0.04 ± 0.00	2	+0.23	-0.03 ± 0.13	3	+0.20	-0.04	+0.22
Na I	6.17	$+0.28 \pm 0.05$	4	+0.56	$+0.19 \pm 0.06$	2	+0.42	+0.24	+0.49
Mg I	7.53	-0.08 ± 0.18	5	+0.20	-0.06	1	+0.17	-0.07	+0.19
Si I	7.51	-0.02 ± 0.13	7	+0.26	$+0.13 \pm 0.16$	10	+0.36	+0.06	+0.31
S I	7.14	$+0.04 \pm 0.13$	5	+0.32	$+0.03 \pm 0.12$	2	+0.26	+0.04	+0.29
Ca I	6.31	-0.18 ± 0.13	20	+0.10	-0.10 ± 0.11	15	+0.11	-0.14	+0.11
Ca II	6.31	-0.15 ± 0.26	2	+0.13	-0.23	1	+0.13	-0.19	+0.13
Sc II	3.05	-0.20 ± 0.07	7	+0.08	-0.35 ± 0.19	7	-0.13	-0.28	-0.03
Ti II	4.90	-0.43 ± 0.13	15	-0.16	-0.50 ± 0.15	7	-0.28	-0.47	-0.22
Cr I	5.64	-0.38 ± 0.11	10	-0.11	-0.55	1	-0.33	-0.47	-0.22
Cr II	5.64	-0.43 ± 0.08	12	-0.16	-0.45 ± 0.13	16	-0.23	-0.44	-0.20
Mn I	5.39	-0.38 ± 0.09	5	-0.11	-0.29 ± 0.11	3	-0.07	-0.34	-0.09
Fe I	7.45	-0.23 ± 0.14	131		-0.18 ± 0.16	97		-0.21	
Fe II	7.45	-0.32 ± 0.12	26		-0.27 ± 0.12	16		-0.30	
Ni I	6.23	-0.28 ± 0.13	11	-0.01	-0.34 ± 0.14	13	-0.12	-0.31	-0.07
Cu I	4.21	-0.61	1	-0.34				-0.61	-0.34
Zn I	4.60	-0.60 ± 0.04	3	-0.33	-0.73	1	-0.51	-0.67	-0.42
Y II	2.21	-0.44 ± 0.13	4	-0.17	-0.43 ± 0.11	5	-0.21	-0.44	-0.19
Zr II	2.59	-0.41 ± 0.15	4	-0.14				-0.41	-0.14
Ba II	2.17	-0.56	1	-0.29	-0.35 ± 0.20	2	-0.13	-0.46	-0.21
La II	1.13	-0.64	1	-0.37				-0.64	-0.37
Ce II	1.58	-0.58 ± 0.12	3	-0.31				-0.58	-0.31

Note. The abundances calculated by synthesis are presented in bold numbers. The rest of the abundances were calculated using line equivalent widths.

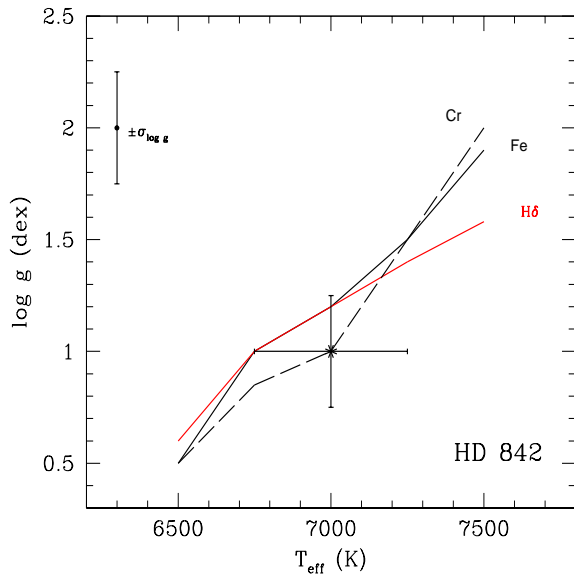


Figure 1. The $H\delta$ and the ionization equilibrium loci for Fe, Cr, Ti and Ca are plotted in temperature gravity plane for HD 842. The asterisk indicates the adopted values of T_{eff} and $\log g$ for the calculation of the atmospheric abundances.

good number of clean lines with similar accuracy to that of OHP spectra. Of course, more care was required in selecting the unblended lines. Although the spectral coverage of VBO

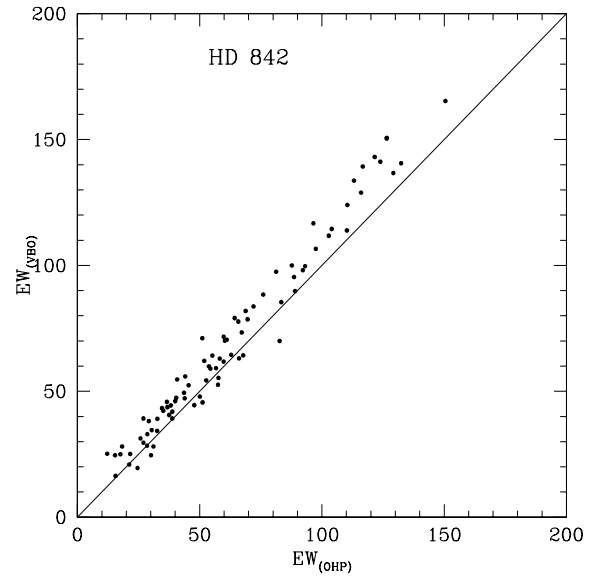


Figure 2. Equivalent widths for lines common between VBO and OHP spectra for HD 842.

echelle is larger (4000 to 9000Å), the number of clean lines used in the abundance were either comparable or smaller than OHP spectrum. For CNO analysis the VBO spectra offered a lot more lines than OHP spectra.

For lines of intermediate strengths to strong lines we

find VBO lines stronger by about 5 to 10%. The two independent atmospheric parameter determination using Fe I and Fe II indicate a higher microturbulence velocity for Sept 22, 2008 epoch by 0.8 km s^{-1} . The temperature and gravity estimates remain unchanged (within the measurement errors). It is not surprising given the lack of reported photometric and radial velocity variations. Our abundance results are presented in Table 4.

It is comforting to see good agreement (within ± 0.2 dex) between the two analyses for most common elements although the number of clean lines measured per element, N, are smaller in 2008 analysis. With most of the program stars having temperatures around 7200K, the 28,000 resolution given by VBO spectra could be used for a satisfactory abundance analysis. Hence we have combined the abundances from the two sets of data for interpretation of the results.

With large number of clean spectral lines available, a satisfactory abundance analysis covering a large number of elements has been carried out. A mild [Fe/H] deficiency of ~ -0.3 dex has been estimated. The [C/H] of -0.3 with a possible NLTE correction of about -0.2 would lead to [C/H] of -0.5 dex and [C/Fe] of -0.2 dex. The [N/H] of $+0.8$ after NLTE correction of -0.3 would imply [N/H] of $+0.5$ and [N/Fe] of $+0.8$ implying conversion of initial carbon into N through CN cycle and products of first dredge-up brought to the surface. At this temperature, the NLTE correction for O would be about -0.1 dex. The observed near-solar O abundance does not indicate ON processing.

A mild enrichment of Na possibly caused by proton capture on ^{22}Ne in H burning region is seen. The α -elements show mild enrichment which is not surprising given the mild [Fe/H] deficiency measured. The elements Sc, Ti, Cr, Mn, Ni show [X/Fe] between -0.09 to -0.22 (not larger than the measurement errors) but Zn shows [X/Fe] of -0.42 dex which defies a simple explanation. The s-process elements appear to be mildly deficient by about -0.2 to -0.3 dex.

4.2 HD 1457

Similar to HD 842, HD 1457 does not have IRAS measurement. The radial velocity measured by Gontcharov (2006) of -44.9 km s^{-1} is somewhat different from the value -35.5 km s^{-1} measured by Grenier et al. (1999). However, we found the radial velocity of $-38.5 \pm 0.3 \text{ km s}^{-1}$ from the OHP spectra obtained on Oct 10, 2000. The two VBO spectra taken on Sept 22, 2008 and Oct 9, 2008 yielded values of -36.1 and -38.2 km s^{-1} respectively. Hence large radial velocity variations are not seen for this star.

Gray, Napier & Winkler (2001) have estimated T_{eff} of 7670K and $\log g$ of 1.7 by fitting low resolution spectra and fluxes at Strömgren filter’s wavelength with the theoretically computed ones. From the line-ratio measurements Kovtyukh (2007) has estimated a temperature of 7636K. The stellar lines appear a little broad indicating a rotation velocity of about 10 km s^{-1} . We arrive at a relatively lower temperature estimate of 7300K based on Fe I/Fe II, Mg I/Mg II, and Ca I/Ca II.

We have used OHP spectra to estimate the atmospheric parameters and also for the abundance analysis. Additional VBO spectra were obtained in 2008 to derive CNO abundances using the lines in red spectral region. However, we

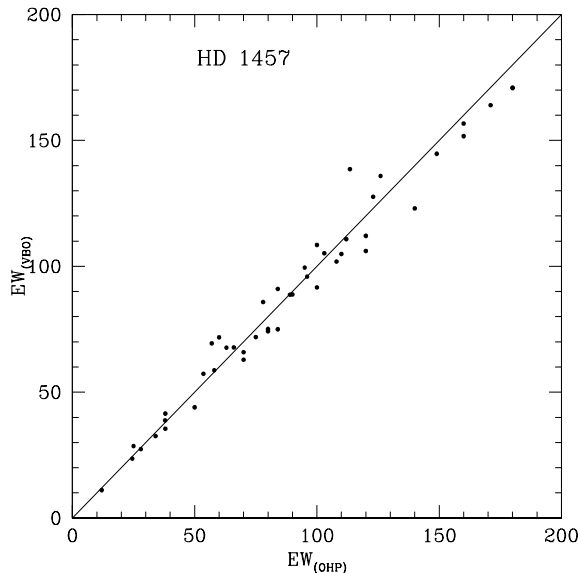


Figure 3. Equivalent widths for lines common between the VBO and OHP spectra for HD 1457.

have compared the line strengths for lines common in both spectra to ensure that there are no variations in atmospheric parameters at these two epochs beyond measurement errors. Fig. 3 gives the comparison of OHP and VBO equivalent widths. It can be seen that the agreement is satisfactory.

A similar sanity check has been conducted for HD 9233 before using the atmospheric parameters derived from OHP spectrum to VBO spectra. Our elemental abundances are presented in Table 5.

Although the star shows near-solar abundance for Fe-peak elements there is significant enrichment of Na relative to Fe. The alpha elements Mg, Ca, Ti are near solar while S exhibits mild enrichment. Na enrichment can be attributed to proton capture on ^{22}Ne in H burning region. Other heavier elements are not significantly different from [X/Fe]=0.

Our CNO abundances are based upon a fairly large number of lines. We derive near solar value of carbon [C/H] -0.25 and [C/Fe] $+0.05$ which with NLTE correction may only imply [C/Fe] of -0.2 . Nitrogen on the other hand shows strong enrichment [N/H] of $+1.55$ and [N/Fe] of 1.75 which even after NLTE correction of -0.4 at 7300K remain much larger than what is expected from complete conversion of initial C to N. With O increasing slightly the excess N cannot be ascribed to ON cycle. The nitrogen enhancement for HD 1457 and other stars of the sample are discussed in section 5.

4.3 HD 9233

This is a high proper-motion star with IR fluxes near the detection limit at IRAS wavelengths. The lines are broad and FWHM indicate a $v \sin i$ of 15 km s^{-1} . The radial velocities on OHP and VBO spectra are -29.9 and -31.9 km s^{-1} respectively. The hydrogen lines have narrow absorption superposed on broad shallow wings. The tip of narrow absorption cores give suggestion of doubling. The diffused interstellar bands at 5870 and 5797Å are very strong indicating that it is a distant object.

Table 5. Elemental abundances for HD 1457.

Specie	$\log \epsilon_{\odot}$	[X/H]	s.d.	N	[X/Fe]
C I	8.39	-0.25	± 0.13	4	-0.06
N I	7.78	+1.55	± 0.02	5	+1.75
O I	8.66	-0.08	± 0.02	2	+0.12
Na I	6.17	+0.51	± 0.15	4	+0.71
Mg I	7.53	-0.14	± 0.06	3	+0.06
Mg II	7.53	-0.06		1	+0.14
Si I	7.51	+0.26	± 0.12	2	+0.46
Si II	7.51	+0.12		1	+0.32
S I	7.14	+0.39	± 0.16	3	+0.59
Ca I	6.31	-0.03	± 0.06	5	+0.17
Ca II	6.31	+0.07	± 0.13	2	+0.27
Sc II	3.05	-0.14	± 0.12	3	+0.06
Ti II	4.90	-0.24	± 0.11	12	-0.05
V II	4.00	-0.23	± 0.01	2	-0.04
Cr I	5.64	-0.31	± 0.10	2	-0.12
Cr II	5.64	-0.19	± 0.15	12	+0.01
Mn I	5.39	-0.21	± 0.00	2	-0.02
Fe I	7.45	-0.18	± 0.11	41	
Fe II	7.45	-0.21	± 0.10	11	
Ni I	6.23	-0.22	± 0.16	5	-0.03
Zn I	4.60	-0.39		1	-0.20
Y II	2.21	-0.40	± 0.13	5	-0.21
Zr II	2.59	-0.24		1	-0.05
Ba II	2.17	-0.22	± 0.22	3	-0.03
La II	1.13	+0.05		1	+0.25
Ce II	1.58	-0.06		1	+0.14

Note. Same as in Table 4.

Due to its relatively hotter temperature, the number of usable lines were relatively few. The atmospheric parameters obtained from the strengths of Fe I and Fe II lines were further confirmed by the loci of Mg I/Mg II, Cr I/Cr II. The elemental abundances are presented in Table 6. The star exhibits very moderate deficiency of [Fe/H] of -0.2 dex. The relative enrichment of Na is similar to that seen in the other stars of this study, deficient Al is hard to explain. The Fe-group elements Ti and Cr show mild deficiencies of about -0.13 to -0.18 dex not larger than measurement errors. A similar moderate deficiency of s-process element is seen. This star again exhibits enhanced nitrogen with [N/H] of $+1.02$. The NLTE correction at this temperature could be about -0.4 dex. The conversion of initial carbon to nitrogen could possibly account for an increased about 0.6 dex but the correspondent decrease in carbon is not very obvious. A more comprehensive analysis involving measurement of $^{12}\text{C}/^{13}\text{C}$ ratio and Al abundance using higher resolution spectra is required to understand this object.

4.4 HD 53300

Parthasarathy & Reddy (1993) pointed out that the IRAS colors of this object were similar to that of Planetary Nebulae (PN) and estimated a dust temperature of 53K and a radius of the dust envelope of 56 to 82 $R_d/R_{\odot} \times 10^5$. The H band spectrum obtained using UKIRT by Oudmaijer et al. (1995) contains only hydrogen absorption lines which is consistent with A0Ib classification.

This A type star has been listed as transition object by

Table 6. Elemental abundances for HD 9233.

Specie	$\log \epsilon_{\odot}$	[X/H]	s.d.	N	[X/Fe]
C I	8.39	+0.04	± 0.05	5	+0.26
N I	7.78	+1.02		1	+1.24
O I	8.66	-0.11	± 0.15	3	+0.10
Na I	6.17	+0.22	± 0.23	2	+0.44
Mg I	7.53	-0.31	± 0.23	4	-0.07
Mg II	7.53	-0.46	± 0.04	2	-0.25
Al I	6.37	-1.57		1	-1.36
Si II	7.51	-0.29	± 0.24	2	-0.08
Ca I	6.31	-0.07	± 0.08	3	+0.15
Ca II	6.31	+0.01	± 0.12	2	+0.23
Sc II	3.05	-0.19	± 0.14	4	+0.03
Ti II	4.90	-0.39	± 0.12	19	-0.18
V II	4.00	-0.34	± 0.22	2	-0.13
Cr I	5.64	-0.39	± 0.15	3	-0.18
Cr II	5.64	-0.38	± 0.14	18	-0.17
Fe I	7.45	-0.20	± 0.15	26	
Fe II	7.45	-0.23	± 0.14	14	
Y II	2.21	-0.29	± 0.06	2	-0.08
Zr II	2.59	-0.59		1	-0.38
Ba II	2.17	-0.39	± 0.17	4	-0.18

Note. Same as in Table 4.

Table 7. Elemental abundances for HD 53300.

Specie	$\log \epsilon_{\odot}$	[X/H]	s.d.	N	[X/Fe]
C I	8.39	-0.83	± 0.18	6	-0.21
N I	7.78	+0.99	± 0.06	5	+1.61
O I	8.66	-0.07	± 0.03	4	+0.57
Na I	6.17	+0.02	± 0.01	3	+0.64
Mg I	7.53	-0.61	± 0.07	5	+0.01
Al I	6.37	-0.96	± 0.12	2	-0.34
Si I	7.51	+0.10	± 0.23	3	+0.72
Si II	7.51	+0.13	± 0.06	2	+0.75
S I	7.14	-0.04	± 0.10	3	+0.58
Ca I	6.31	-0.69	± 0.14	9	-0.07
Ca II	6.31	-0.55	± 0.01	2	+0.07
Sc II	3.05	-0.96	± 0.16	14	-0.34
Ti II	4.90	-0.83	± 0.14	55	-0.21
V II	4.00	-0.89	± 0.15	7	-0.27
Cr II	5.64	-0.63	± 0.14	33	-0.01
Mn I	5.39	-0.01		1	+0.61
Fe I	7.45	-0.61	± 0.14	81	
Fe II	7.45	-0.63	± 0.13	54	
Ni I	6.23	-0.59		1	+0.03
Ni II	6.23	-0.71	± 0.06	3	-0.09
Zn I	4.60	-0.71		1	-0.09
Sr II	2.92	-1.68		1	-1.06
Y II	2.21	-1.28	± 0.17	3	-0.66
Zr II	2.59	-0.90	± 0.13	5	-0.28
Ba II	2.17	-1.12	± 0.14	3	-0.50

Ortiz et al. (2005) who have been studying post-AGB and PNe using the MSX survey data.

The optical linear polarization of $1.0\% \pm 0.13$ has been reported by Bhatt & Manoj (2000) which is much larger than ISM value and these authors explain the observed polarization to the scattering of light due to circumstellar matter distributed in non-spherically symmetric envelopes possibly distributed in the flattened disk.

The Strömgen photometric indices c_1 , m_1 and $u - v$

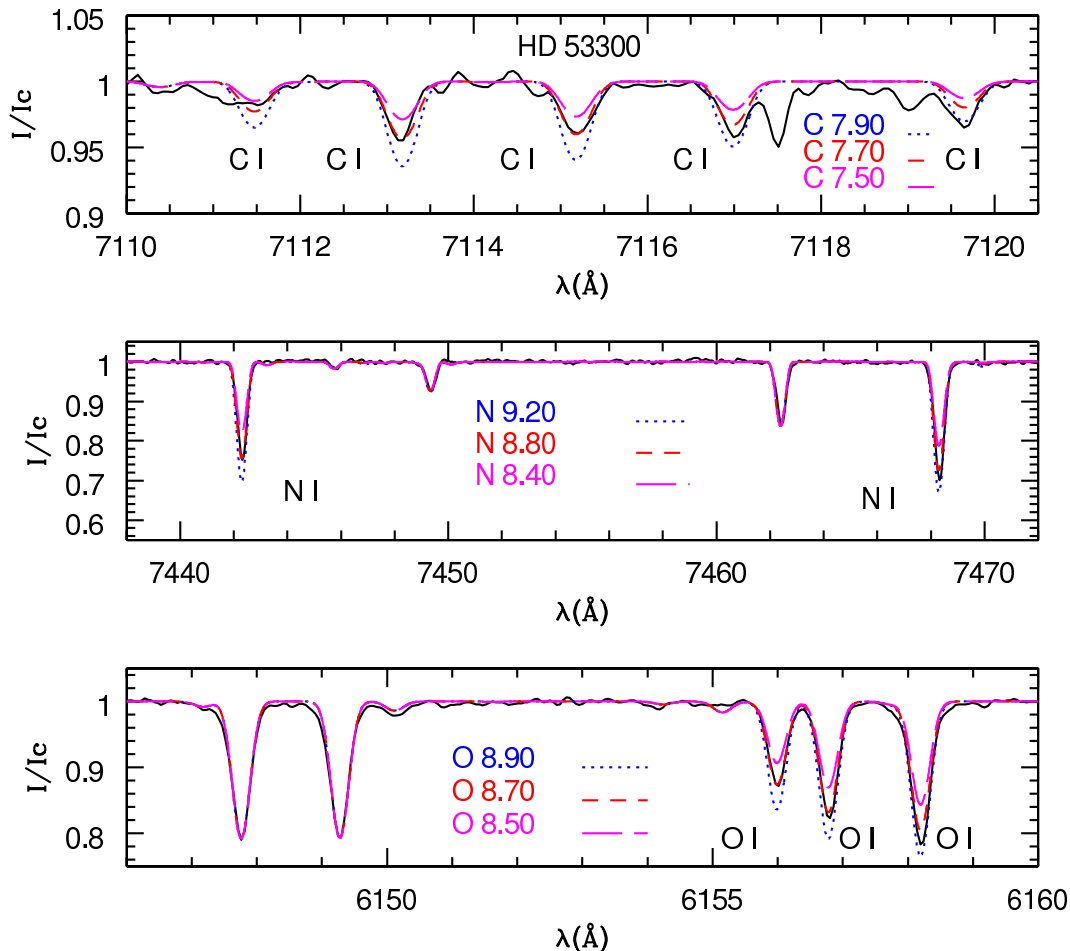


Figure 4. The agreement between the synthesized and observed spectrum for spectral regions containing CNO lines for HD 53300.

translate to a temperature of 7200K, while spectral type A0Ib when used with the calibration of Schmidt-Kaler (1982) yield a temperature of 8500K.

The radial velocity of the star measured from the spectrum taken on Feb 18, 2006 was $+58.3 \pm 0.6 \text{ km s}^{-1}$ while for the spectrum taken on Nov 2, 2007 was $+58.4 \pm 0.6 \text{ km s}^{-1}$.

For the abundance analysis of this star we have used a spectrum obtained at the McDonald Observatory 2.7m telescope equipped with 2D coude spectrograph giving a resolution of 60,000 and continuous spectral coverage over 3800-10000Å in a single CCD frame.

Our atmospheric parametrization based upon a very large number of Fe I and Fe II lines is also supported by the ionization equilibrium study of Mg I/Mg II, Si I/Si II and Ca I/Ca II. The elemental abundances are presented in Table 7.

The spectrum of the star is not crowded but contains a large number of lines for several important elements. We derive atmospheric parameters T_{eff} 7500K, $\log g$ of 0.5, microturbulent velocity of 2.4 km s^{-1} and $v \sin i$ of 10 km s^{-1} . The star is moderately metal-poor with $[\text{Fe}/\text{H}]$ of -0.6 dex. The metallicity and moderately high radial velocity pointed to the possibility of thick disk population, hence a comparison has been made with the abundance trends seen in thick disk stars (Reddy, Lambert & Allende Prieto 2006).

HD 53300 shows relative enrichment of sodium possibly caused by proton capture on ^{22}Ne . The α elements do not show a consistent enrichment relative to Fe of +0.3 dex expected for the thick disk; $[\text{Si}/\text{Fe}]$ and $[\text{S}/\text{Fe}]$ show much larger values of +0.7 and +0.6 while $[\text{Mg}/\text{Fe}]$ is +0.01, $[\text{Ca}/\text{Fe}]$ of 0.0 and $[\text{Ti}/\text{Fe}]$ of -0.2 . The $[\text{Al}/\text{Fe}]$ of -0.4 is lower than the expected value for the thick disk. The Fe-peak elements $[\text{Ni}/\text{Fe}]$, $[\text{Zn}/\text{Fe}]$ are near zero but s-process elements exhibit deficiencies ranging from -0.3 dex for Zr to -0.7 dex for Y.

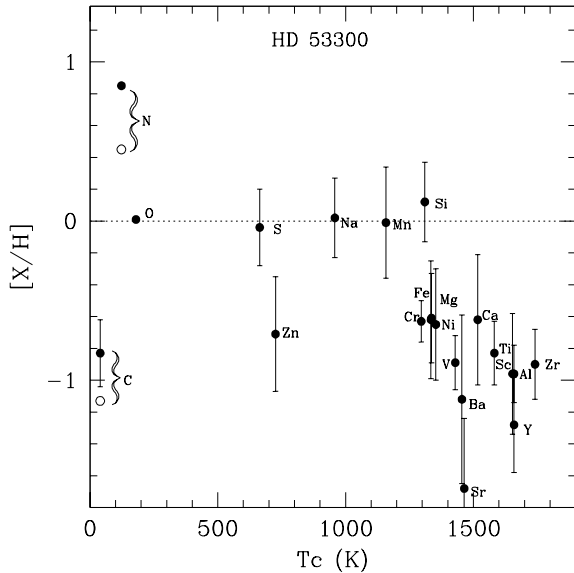
The abundance pattern of HD 53300 shows selective depletion of refractory elements first observed in HR 4049 (Lambert, Hinkle & Luck 1988). The abundance anomalies of these stars are roughly correlated with the predicted condensation temperature for low pressure gas of solar composition. Hence, elements like Al, Ca, Ti and Sc with the highest condensation temperatures (1500 to 1600K) would be significantly depleted while the elements with low condensation temperatures (like S, Zn) would not be affected.

A similar effect for RV Tau star IW Car had been reported by Giridhar, Kameswara Rao & Lambert (1994) which was later seen in many RV Tau stars (see Giridhar et al. 2005 for a summary) and post-AGB stars (see van Winckel 2003 for an extensive review). Condensation temperature T_C is defined as the temperature, at which 50 %

Table 8. Elemental abundances for HD 61227.

Specie	$\log\epsilon(X)_{\odot}$	OHP (Oct 7 2000) (7000,1.0,4.0)			VBO (Feb 12 and 18, 2006) (7000,1.0,4.0)			Average	
		[X/H]	N	[X/Fe]	[X/H]	N	[X/Fe]	[X/H]	[X/Fe]
C I	8.39	-0.40 ± 0.3	3	-0.04	-0.31 ± 0.14	9	+0.09	-0.35	$+0.03$
N I	7.78				$+0.67 \pm 0.10$	4	+1.07	$+0.67$	$+1.07$
O I	8.66	-0.33	1	+0.03	-0.32	1	+0.08	-0.33	$+0.06$
Na I	6.17	$+0.13 \pm 0.05$	2	+0.49	+0.17	1	+0.57	+0.15	+0.53
Mg I	7.53	-0.40 ± 0.21	3	-0.04	-0.35 ± 0.02	2	+0.05	-0.38	+0.01
Si I	7.51	-0.15		+0.21	-0.14 ± 0.20	5	+0.26	-0.15	+0.24
S I	7.14	$+0.03 \pm 0.03$	2	+0.39				+0.03	+0.39
Ca I	6.31	-0.33 ± 0.15	9	+0.03	-0.28 ± 0.14	11	+0.12	-0.31	+0.08
Ca II	6.31	-0.15	1	+0.21				-0.15	+0.21
Sc II	3.05	-0.35 ± 0.19	6	+0.01	-0.16 ± 0.18	5	+0.24	-0.18	+0.13
Ti II	4.90	-0.49 ± 0.15	11	-0.13	-0.49 ± 0.18	9	-0.10	-0.49	-0.12
V II	4.00	-0.30	1	+0.06	-0.34	1	+0.06	-0.32	+0.06
Cr I	5.64	-0.40 ± 0.16	7	-0.04	-0.47 ± 0.05	5	-0.08	-0.44	-0.06
Cr II	5.64	-0.44 ± 0.15	12	-0.08	-0.40 ± 0.20	11	-0.01	-0.42	-0.04
Mn I	5.39	-0.60 ± 0.17	2	-0.24	-0.49 ± 0.11	2	-0.10	-0.55	-0.17
Fe I	7.45	-0.38 ± 0.15	66		-0.33 ± 0.16	84		-0.36	
Fe II	7.45	-0.34 ± 0.13	14		-0.46 ± 0.13	10		-0.40	
Co I	4.92	-0.54	1	-0.18				-0.54	-0.18
Ni I	6.23	-0.36 ± 0.11	8	+0.00	-0.38 ± 0.13	10	+0.02	-0.37	+0.01
Zn I	4.60				-0.47 ± 0.01	2	-0.08	-0.47	-0.08
Y II	2.21	-0.40 ± 0.16	2	-0.04	-0.47 ± 0.15	4	-0.08	-0.44	-0.06
Zr II	2.59	-0.23 ± 0.11	3	+0.13	-0.41	1	-0.02	-0.34	+0.08
Ba II	2.17	-0.44	1	-0.08	-0.28 ± 0.05	2	+0.12	-0.36	+0.02
La II	1.13	-0.35 ± 0.04	2	+0.01				-0.35	+0.01
Ce II	1.58	-0.15 ± 0.10	3	+0.21	-0.30 ± 0.05	2	+0.10	-0.23	+0.16
Nd II	1.45				-0.30 ± 0.07	2	+0.10	-0.30	+0.10

Note. Same as in Table 4.

**Figure 5.** Abundance [X/H] versus condensation temperature T_C for HD 53300. Open circles indicate the C and N values after the correction for NLTE.

gas is condensed into solid form as estimated for solar system abundances and a pressure of 10^{-4} bar. We have plotted the estimated [X/H] as a function of condensation temperatures T_C (the T_C data is taken from Lodders 2003) in Fig. 5. The

observed CNO are affected by nucleosynthesis and mixing episodes. But for the rest the pattern is quite obvious, the elements with T_C larger than 1250K show depletion correlated with T_C . The low condensation elements (with the exception of Zn) S, Na, Mn, Si are unaffected.

We have shown in Fig. 4 the agreement between the synthesized and observed spectrum for spectral regions containing CNO lines for HD 53300. The star has under abundances of carbon ($[C/H] = -0.8$) and a NLTE correction of -0.3 dex at this temperature would imply $[C/H]$ of -1.1 . The nitrogen abundance is $[N/H] = +0.99$ and $[N/Fe]$ of 1.61. At the temperature of 7500K the NLTE correction could be -0.4 dex, hence $[N/H] = +0.59$ and $[N/Fe]$ of $+1.21$ imply N production in excess of CN process. The $[C/Fe]$ of -0.2 for HD 53300 is not very instructive since the Fe abundance is affected by depletion. However, S which is a better indicator of metallicity, shows near-solar value hence we consider the derived $[C/H]$ and $[N/H]$ values. The observed reduction of C and excess increase of N could point towards possible HBB operating in AGB stars more massive than $5M_{\odot}$. However, we do not see the Li enhancement predicted by HBB.

HD 53300 therefore belongs to the family of post-AGB stars showing depletion of condensable elements.

4.5 HD 61227

This high proper motion star has weak IR fluxes almost at the detection limit for IRAS filters. The temperatures

have been estimated from different approaches. A temperature of 7433K has been estimated using the line ratios of temperature sensitive lines by Kovtyukh (2007). From the Strömrgren photometry, Gray & Olsen (1991) estimate temperature of 7267K; however, the spectral type of F0Ib may indicate a higher temperature of 7700K. The temperature derived by us is in good agreement with that derived from Strömrgren photometry. Rotation velocity of 10 and 18 kms^{-1} has been reported by Royer et al. (2002), Abt & Morell (1995). It has been included in several radial velocity projects e.g. Beavers & Eitter (1986), the Pulkovo Compilation by Gontcharov (2006). We have also derived radial velocity for several epochs and our estimates are presented in Table 2. We do not notice a significant variation in the radial velocities measured.

We had one OHP spectrum of this star taken in 2000 and several in 2006 using echelle spectrometer of VBO. We have made two independent analyses of the spectra taken in 2000 and those in Feb 2006. Table 8 gives the derived abundances. The star appears to show moderate deficiency of Fe of -0.38 dex and a mild deficiency of ~ -0.4 dex seen for Ti, Ni and Cr. S and Si show near solar values. The mean carbon abundances from individual lines in these analyses gives $[\text{C}/\text{H}]$ of -0.35 and $[\text{C}/\text{Fe}]$ of $+0.03$. At 7000K the NLTE correction could be about -0.2 , hence NLTE estimate of $[\text{C}/\text{H}]$ of -0.55 dex and $[\text{C}/\text{Fe}]$ of -0.17 . The estimated $[\text{N}/\text{H}]$ of $+0.67$ shows significant overabundance even with a NLTE correction of -0.4 which implies $[\text{N}/\text{H}]$ of $+0.27$ or $[\text{N}/\text{Fe}]$ of $+0.65$. The oxygen abundance $[\text{O}/\text{H}]$ of -0.33 , after NLTE correction of -0.15 implies $[\text{O}/\text{H}]$ of -0.48 or $[\text{O}/\text{Fe}]$ of -0.10 . There are indication of CN processing in the form of increased nitrogen possibly caused by conversion of initial carbon into nitrogen and the product of CN processes are dredged up to the surface.

4.6 HD 105262

This object has been included in Torun catalogue of post-AGB and related objects under the class of High Galactic Latitude Supergiants due to its galactic latitude of $+72.47^\circ$, and supergiant characteristics. Being a relatively bright object ($V=7.08$), several estimates of atmospheric parameters and radial velocities have been reported. The compilation of rotational velocity in metal-poor stars by Cortes et al. (2009) gives following atmospheric parameters $T_{\text{eff}}=8855\text{K}$, $\log g=1.82$ cgs and $v \sin i=6.1 \text{ kms}^{-1}$. It is included in the Catalogue of $[\text{Fe}/\text{H}]$ determination by Cayrel de Strobel et al. (1992) which gives $T_{\text{eff}}=8550\text{K}$, $\log g=1.5$ in cgs, and $[\text{Fe}/\text{H}]=-1.37$ using high resolution spectra and differential curve-of-growth analysis relative to a star of similar atmospheric parameters. Klochkova & Panchuk (1987) have estimated $T_{\text{eff}}=8500\text{K}$, $\log g=1.5$ employing Balmer line profile fits. Martin (2004) had estimated a starting value of $T_{\text{eff}}=8819\text{K}$ from Johnson colours $(B-V)=-0.01$ when used with colour temperature relation of Napiwotzki, Schönberner, & Wenske (1993) and $T_{\text{eff}}=9240\text{K}$ from Strömrgren $[u-b]$ color and calibration of Napiwotzki, Schönberner, & Wenske (1993). He, however derived $T_{\text{eff}}=9000\text{K}$, $\log g=2.50$, $\xi=2.0 \text{ kms}^{-1}$, $[\text{Fe}/\text{H}]=-1.54$ and $v \sin i$ of 6.0 kms^{-1} using high resolution spectra and model atmospheres.

There are several radial velocity estimates for this star.

A radial velocity of $+31.1 \text{ kms}^{-1}$ has been reported by Gontcharov (2006) and $+43.6 \text{ kms}^{-1}$ by Grenier et al. (1999), and $+41.4 \text{ kms}^{-1}$ by Duflot et al. (1995) while our spectrum taken on May 10, 2009 gave a radial velocity of $+67.3 \text{ kms}^{-1}$ hence a significant variation in radial velocity is indicated.

This star was considered a Field Horizontal Star (FHB) by Glaspey (1982). However, using a medium resolution spectra, Reddy, Parthasarathy & Sivarani (1996) have shown that for this star the hydrogen lines are much narrower than those FHB stars and are more like those of A type supergiants. From their analysis, they reported this star to be a C-rich post-AGB star of low metallicity. This star was included in the study of high galactic latitude B stars using high resolution spectra by Martin (2004) as possible post-AGB star. However, the carbon enrichment reported by Reddy, Parthasarathy and Sivarani (1996) has not been confirmed. In fact, Martin (2004) does not give even the upper limit for C, N abundances but report only estimates for abundances of a few Fe-peak elements. We have attempted a more comprehensive study of this star using a high resolution spectrum obtained with 2.7m Harlan J. Smith reflector and 2dcoude echelle spectrometer giving a resolution of 60,000. The S/N ratio is 50.

The $\text{H}\alpha$ line has a deep absorption component superposed on a broader much shallower component. The $\text{H}\beta$ profile is similar but the contrast between deep narrow absorption and broad shallow one is reduced. The $\text{H}\gamma$ and $\text{H}\delta$ appear similar to those seen in A-type supergiants. The He I lines at 4471 and 4713Å are very weak with equivalent widths of 38 and 12mÅ respectively. The metal lines are indeed very weak, in fact most of them lie on the linear portion of the curve-of-growth and hence are not sensitive to microturbulence. The metal lines are quite sharp and we confirm low rotation velocity of 6 kms^{-1} estimated earlier by Martin (2004). We could still measure sufficient number of lines of the Fe-group elements. For the α elements only a few lines were available. The Na and Ca abundances are based upon a very weak feature and should be considered as lower limits. With the extended coverage in red, we could measure four lines of N I. We have used three O I lines in 6156-58Å region to derive oxygen abundance. The search for C I, C II lines has not been successful. Even the strongest line of C I at 9094.89Å could not be measured indicating a very large under abundance of carbon. At the temperature of 8500K, the lines of S I were also very difficult to detect, the strongest feature at 6757.17Å could be seen as a weak feature of about 2.0mÅ strength. The estimate for S abundance therefore is a limiting value.

We estimate a $T_{\text{eff}}=8500\text{K}$, $\log g=1.50$ in csg, $\xi=2.8 \text{ kms}^{-1}$ based upon Fe I and Fe II lines. Another possible solution could be $T_{\text{eff}}=8750\text{K}$, $\log g=2.00$. Given the relatively high temperature estimates from the photometry, we chose to present the results for these two temperatures in the Table 9 although the abundance trends are the same for the two sets. However, a satisfactory fit to $\text{H}\gamma$ could be obtained with $T_{\text{eff}}=8500\text{K}$, $\log g=1.50$ as shown in Fig. 6.

The light elements N I and O I show considerable enhancement while carbon is severely under-abundant with $[\text{C}/\text{H}]$ less than -3.0 . With $[\text{Fe}/\text{H}]$ of -1.8 , this star is at odds with young B supergiants. The $[\text{X}/\text{Fe}]$ of α elements Mg, Si, Ti appear to be similar to those seen in metal-poor stars but $[\text{X}/\text{Fe}]$ of N, O, Ca, Sc and Cr are quite different.

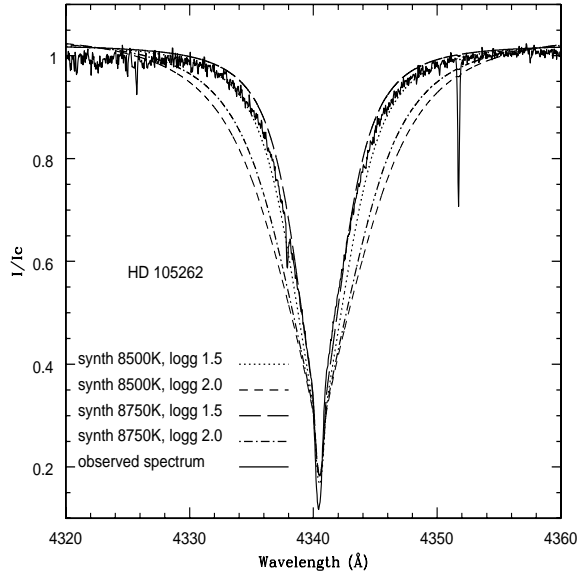


Figure 6. $H\gamma$ profile for HD 105262 compared with several models.

With existing uncertainty in the distance for this object, it is difficult to say how far above the galactic plane this object is situated. The Blue Metal-Poor (BMP) tend to be Main Sequence objects ($\log g$ 4.0 to 4.5 Preston & Sneden 2000) while HD 105262 has $\log g$ of 1.5. On the other hand, the abundances of this star resemble those of hot post-AGB star studied by Conlon et al. (1993, 1994), McCausland et al. (1992). We have plotted in Fig. 7 the observed $[X/H]$ as a function of condensation temperature (T_c) for this as well as other hot post-AGB stars. The light elements C, N, O are not much affected by condensation but reflect the changes caused by CN processing, although ultra low carbon abundances are hard to explain through CN processing alone. Intermediate depletion shown by Mg, Si and largest depletion shown by Ca and Sc follows the expected dependence on T_c . A similar trend is also exhibited by HD 137569 and ROA 5701 although for these objects the analysis contains fewer elements. HD 105262 appears to be a cooler analogue of hot post-AGB stars showing depletion of refractory elements.

BD+39°4926 and HD 137569 are well-known examples of post-AGB binaries without IR excesses. The radial velocities obtained for HD 105262 display large enough variations (+31.1, +41.1, +43.6 and +67.3 kms^{-1}) to support the possibility of this being a binary star and should be included in the radial velocity campaign.

4.7 CpD-62°5428

This high galactic latitude A supergiant star is also known as IRAS 16399-6247. With [12]-[25] color of +1.7 and [60]-[100] of 0.4, it belongs to the zone of very likely post-AGB stars defined by van der Veen & Habing (1988). Its galactic latitude is -11.1° and exhibits a modest radial velocity of -29.9 kms^{-1} . The $H\alpha$ has narrow inverse P-Cygni structure at the line centre superposed on the broad absorption and emission rises above continuum level. The central emission is not strong enough to rise above the continuum in $H\beta$ but is

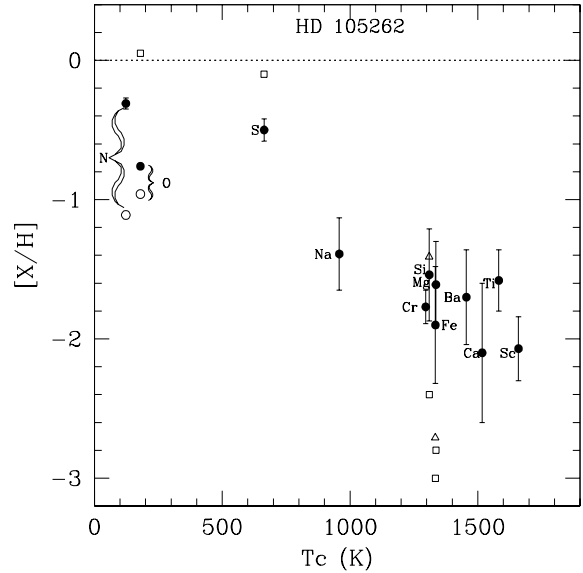


Figure 7. Abundance $[X/H]$ versus condensation temperature for HD 105262 (filled circles). We have also included the abundance of the hot post-AGB stars HD137569 (empty squares) (Giridhar & Arellano Ferro 2005) and ROA 5701 (empty triangles) (Moehler et al. 1998). Open circles indicate the N and O values after the correction for NLTE.

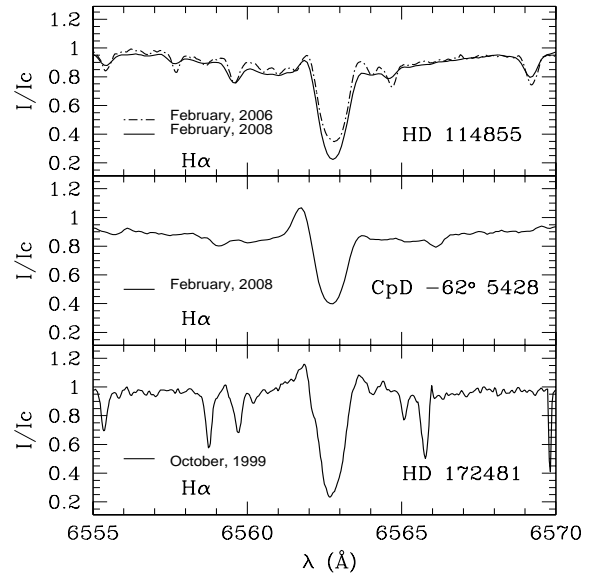


Figure 8. $H\alpha$ profiles in HD 114855, CpD $-62^\circ 5428$ and HD 172481.

perceptible as asymmetry in the central narrow absorption. Other lines of hydrogen also show the indication of filling in by the central emission, hence hydrogen lines could not be used to estimate the atmospheric parameters.

The $H\alpha$ profiles in post-AGB stars show a range in emission-absorption structure related to the complex atmospheric motions. Spectroscopic monitoring of $H\alpha$, Na I D lines had been undertaken by Kwok et al. (1990) for HD 56126 (a well known post-AGB star) who found inverse P-Cygni and shell like profile in the same night. A long

Table 9. Elemental abundances for HD 105262.

Specie	$\log\epsilon(X)_\odot$	(8500,1.5,2.8)			(8750,2.0,2.8)		
		[X/H]	N	[X/Fe]	[X/H]	N	[X/Fe]
N I	7.78	-0.31 ± 0.19	4	+1.59	-0.27 ± 0.19	4	+1.51
O I	8.66	-0.76 ± 0.04	3	+1.14	-0.73 ± 0.04	3	+1.05
Na I	6.17	-1.39	1	+0.51	-1.39	1	+0.39
Mg I	7.53	-1.61 ± 0.03	2	+0.29	-1.59 ± 0.03	2	+0.19
Si I	7.51	-1.70	1	+0.20	-1.65	1	+0.13
Si II	7.51	-1.37 ± 0.27	5	+0.53	-1.23 ± 0.23	5	+0.55
S I	7.14	-0.50	1	+1.40	-0.51	1	+1.27
Ca I	6.31	-2.10	1	-0.20	-2.10	1	-0.32
Sc II	3.05	-2.07	1	-0.17	-1.89	1	-0.11
Ti II	4.90	-1.58 ± 0.14	26	+0.32	-1.40 ± 0.14	26	+0.38
Cr II	5.64	-1.77 ± 0.18	8	+0.13	-1.61 ± 0.18	8	+0.17
Fe I	7.45	-1.93 ± 0.10	9		-1.87 ± 0.10	9	
Fe II	7.45	-1.87 ± 0.11	28		-1.69 ± 0.11	28	
Ba II	2.17	-1.70	1	+0.20	-1.68	1	+0.10

term monitoring of this star by Oudmaijer & Bakker (1994) report variations in the profile over time scales of 30–96 days. A more comprehensive study of this object by L ebre et al. (1996) included the profile variations of $H\alpha$ as well as other strong atomic lines over an year. These authors also found that $H\alpha$ profiles changes from P–Cygni, reverse P–Cygni profile, Shell profile to asymmetric absorption. L ebre et al. (1996) reported that $H\alpha$ profile changes from one type to another in the time scale of a few days. The observed $H\alpha$ profile for CpD–62°5428, HD 114855 and HD 172481 (studied by Arellano Ferro, Giridhar & Mathias 2001) are presented in Fig. 8. It is generally believed that P–Cygni like profile structure is caused by the presence of shock propagating in the pulsating atmosphere of these stars. From the observations that at some phases the blue shifted, or red shifted, or both side emission components above the continuum are seen, L ebre et al. (1996) propose that single broad shock emission is modified by an almost central absorption. Depending upon the wavelength of absorption relative to shock emission, the resultant double emission peaked profile would have stronger blue shifted or red shifted components. Such profiles are reported in a few RV Tau and W Vir stars by L ebre & Gillet (1992) and Fokin (1991).

Remarkably little work has been done for this object. Although the SIMBAD search revealed a reference to the Torun catalog of post-AGB objects (Szczerba et al. 2007), it does not belong to any of the three tables contained in the catalogs. The photometric information is restricted to the broad band *BVRIJ* colors and fluxes at IRAS wavelengths. In the absence of any other information, the atmospheric parameters are determined using the excitation and ionization equilibrium of atomic lines of Fe, Si, Mg and Cr. The star being of spectral type A, the spectrum is not crowded and large number of lines for many species in neutral and first ionized state could be measured. We could measure 191 lines of Fe I and 45 lines of Fe II. Our CNO abundances are also based upon a fairly large number of lines made possible by the extended spectral coverage of the MIKE spectrograph at LCO. The derived abundances are presented in Table 10. The star is moderately metal-poor with [Fe/H] of -0.4 dex.

We have shown in Fig. 9 the agreement between the

synthesized and observed spectrum for spectral regions containing CNO lines for CpD–62°5428.

The carbon abundance is derived using lines in 4770–75Å, 6013–20Å and 7110–15Å region. A near-solar carbon abundance [C/H] +0.09 is found, which with a -0.2 dex NLTE correction at this temperature may imply [C/H] of -0.1 dex, which is larger than the 1st dredge up predictions hence indicating the replenishment of carbon through triple α reactions. The NLTE corrected values of carbon and oxygen abundances indicate a C/O of ~ 0.4 . Even after applying the NLTE correction of -0.4 dex, N is still enhanced and points to the total conversion of initial C to N.

Since [Fe/H] of -0.4 is similar to that of the thick disk component, we chose to compare our derived abundances with those estimated for the thick disk by Reddy et al. (2006). The relative enrichment of Na ([Na/Fe] of +0.56) is larger than the thick disk value of +0.12 dex at -0.5 [Fe/H]. Its over-abundance may be caused by proton capture on ^{22}Ne in the hydrogen burning stage.

The behaviour of α elements is not fully compatible to the thick disk values. The derived [Mg/Fe] of +0.2 dex and [Si/Fe] of +0.3 dex are similar to those expected for thick disk stars but the derived [S/Fe] of +0.5 is larger and [Ca/Fe] of -0.1 dex and [Ti/Fe] of -0.2 dex are lower than expected thick disk values. More significant differences are shown by [Al/Fe] of -0.8 and [Sc/Fe] of -0.2 dex which are +0.3 dex and +0.2 dex respectively for the thick disk. The s-process elements show significant deficiency while [s/Fe] of nearly zero is expected for the thick disk. However the observed abundance pattern has close resemblance to that seen in post-AGB stars with C/O nearly one or less.

We have plotted in Fig. 10 the observed abundances for CpD –62°5428 as function of the condensation temperatures for the elements (Lodders 2003). The depletion pattern is obvious, although the size of depletion (can be measured through [X/H] for Al, Sc, Ti) is modest. It is tempting to ascribe the deficiency to dust condensation but the scatter in the [X/H] vs T_C led us to explore other possibilities. It is possible that additional processes are operating. Another possible explanation is based upon First Ionization Potential (FIP) effect initially seen in solar chromosphere and corona

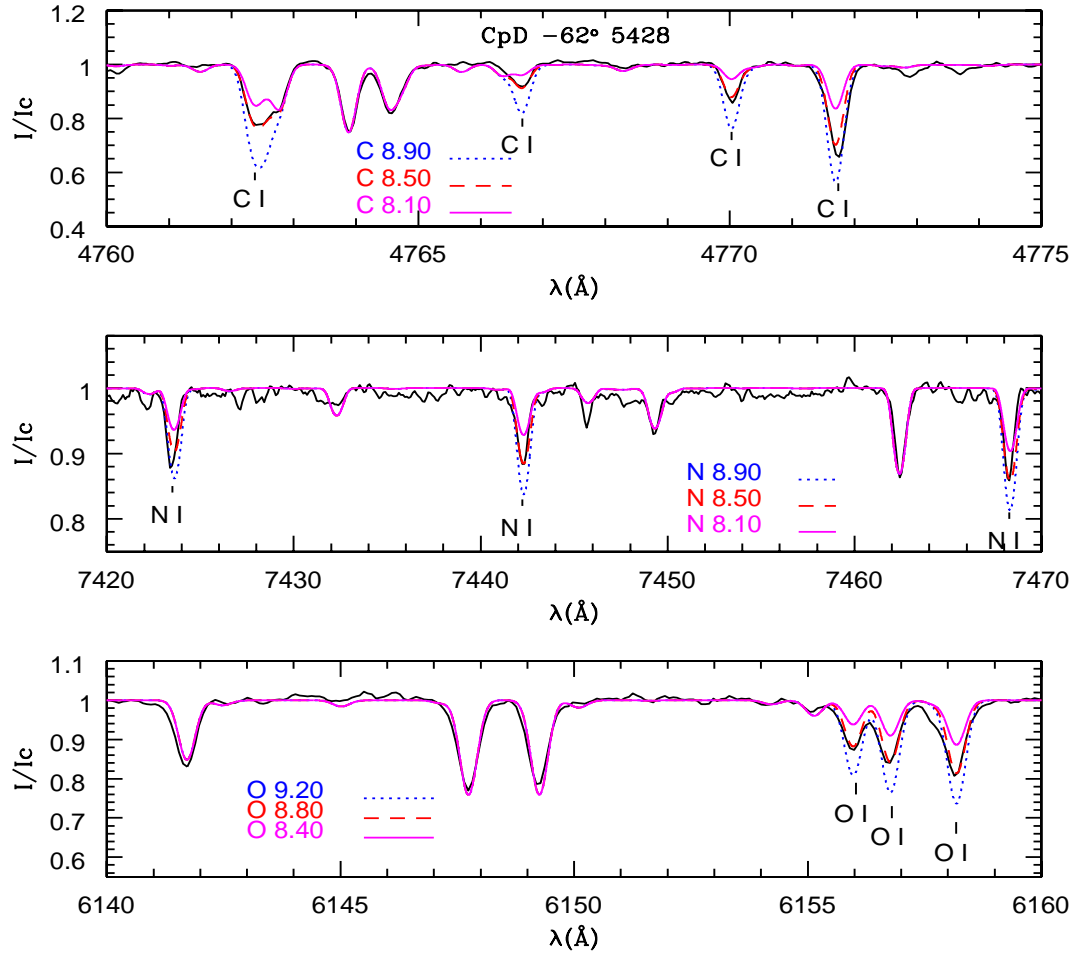


Figure 9. The agreement between the synthesized and observed spectrum for spectral regions containing CNO lines for CpD $-62^{\circ}5428$.

where ions of low FIP elements rather than neutral atoms are fed from the chromosphere to corona. Kameswara Rao & Reddy (2005) found strong dependence of elemental depletion on their FIP for CE Vir and EQ Cas. These authors propose that singly ionized elements escaped as stellar wind rather than being coupled to the radiation pressure on the dust.

We have plotted $[X/H]$ vs. FIP in Fig. 11 for CpD $-62^{\circ}5428$ and we find that for elements with FIP lower than 8eV, there is a good correlation with the exception of Na. However, we need a mechanism to power the wind (Shock to generate high energy photons?). The star has been monitored for about 8 years by the All Sky Automated Survey (ASAS) group. The light curve includes 571 observations and does not show signs of a systematic variation, but a scatter of about ± 0.2 mag and occasional "drop-outs" of 0.3 to 0.8 mag which in our opinion are spurious. A long term profile monitoring of lines such as H α need to be carried out to detect the passage of the shock.

4.8 HD 114855

This southern star with robust detection in IRAS 25, 60, 100 μ bands has been included in many studies of AGB and PN like sources. Parthasarathy & Reddy (1993) have reported a

cool dust of temperature 70K. Walker & Wolstencroft (1988) have modeled the available fluxes to derive stellar and dust parameters for a sample of Vega like stars. These authors estimate a temperature of 6350K for the star, and the dust temperature of 95K. A radial velocity of $-5.6 \text{ km s}^{-1} \pm 0.4 \text{ km s}^{-1}$ has been given Gontcharov (2006). de Medeiros et al. (2002) give the same radial velocity but also rotational velocity $v \sin i$ of 12.2 km s^{-1} . Photometric variations are reported by Koen & Eyer (2002) with amplitude of variation of ~ 0.074 mag. Kazarovets et al. (1999) also report light variation with V_{max} of 8.57 and V_{min} of 9.15. We have several spectra of this objects taken in the last 2 years. As indicated in Table 2, we notice a range in radial velocity of -13.6 to $+73.0 \text{ km s}^{-1}$. The hydrogen lines are distorted due to the presence of emission. However preliminary estimates of temperature based on Strömgren photometry range from 6600K to 6400K. We however, find a temperature of 6000K and $\log g$ of 0.5 based upon the excitation and ionization equilibrium of Fe I/Fe II, Cr I/Cr II, Ti I/Ti II and Si I/Si II. The star contains a remarkably large number of C I lines and the N I lines are also strong. The elemental abundances are presented in the Table 11. The CNO abundances again not only show the influence of CN processing converting initial carbon to nitrogen but mixing of triple alpha processed carbon to convective envelope is also indicated.

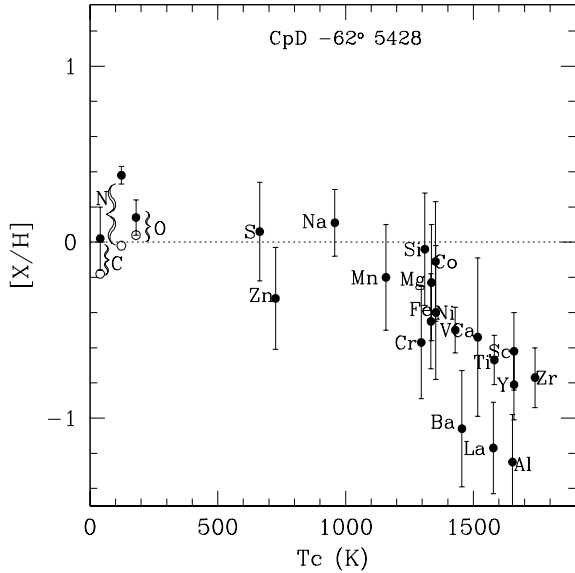


Figure 10. Abundance $[X/H]$ versus condensation temperature for CpD $-62^\circ 5428$

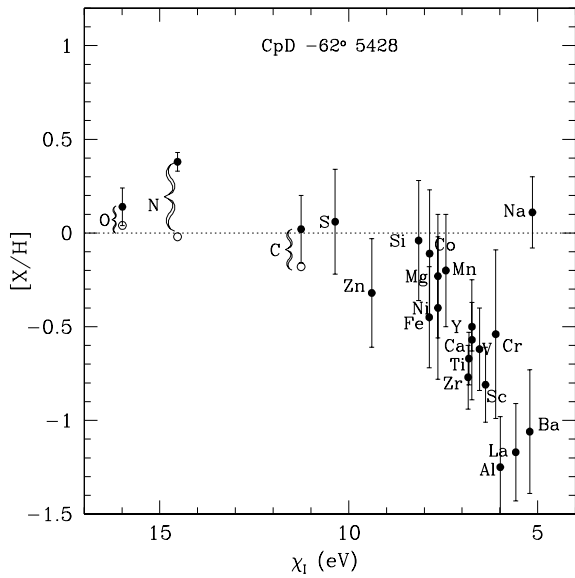


Figure 11. Abundance $[X/H]$ versus First Ionization Potential in eV for CpD $-62^\circ 5428$

This star shows very mild signature of dust-gas separation. The low condensation element S shows mild enrichment, Zn is nearly solar while easily condensable elements Sc, Ca are depleted. Similarly, the s-process elements show stronger depletions. The depletion pattern is presented in Fig. 12 but the magnitude of depletion is very modest.

The observed abundance peculiarities, IR detection and observed large variations in the radial velocity for this star makes it a very likely post-AGB star with a binary companion and deserves radial velocity and profile monitoring.

Table 10. Elemental abundances for CpD $-62^\circ 5428$.

Species	$\log \epsilon_\odot$	$[X/H]$	s.d.	N	$[X/Fe]$
C I	8.39	+0.02	± 0.13	6	+0.47
N I	7.78	+0.38	± 0.18	3	+0.83
O I	8.66	+0.14	± 0.07	3	+0.59
Na I	6.17	+0.11	± 0.08	3	+0.56
Mg I	7.53	-0.20	± 0.07	6	+0.25
Mg II	7.53	-0.25		1	+0.20
Al I	6.37	-1.25	± 0.03	2	-0.80
Si I	7.51	+0.07	± 0.16	4	+0.52
Si II	7.51	-0.15	± 0.02	2	+0.16
S I	7.14	+0.06	± 0.15	2	+0.47
Ca I	6.31	-0.54	± 0.11	14	-0.09
Ca II	6.31	-0.54		1	-0.09
Sc II	3.05	-0.62	± 0.20	11	-0.17
Ti II	4.90	-0.67	± 0.14	39	-0.22
V II	4.00	-0.50	± 0.14	12	-0.05
Cr I	5.64	-0.57	± 0.16	7	-0.12
Cr II	5.64	-0.56	± 0.14	27	-0.11
Mn I	5.39	-0.24	± 0.22	3	+0.21
Mn II	5.39	-0.16		1	+0.29
Fe I	7.45	-0.45	± 0.12	191	
Fe II	7.45	-0.45	± 0.11	45	
Co I	4.92	-0.11	± 0.08	3	+0.34
Ni I	6.23	-0.36	± 0.16	9	+0.09
Ni II	6.23	-0.44		1	+0.01
Zn I	4.60	-0.32		1	+0.13
Y II	2.21	-0.81	± 0.15	10	-0.36
Zr II	2.59	-0.77	± 0.13	7	-0.32
Ba II	2.17	-1.06	± 0.16	5	-0.61
La II	1.13	-1.17		1	-0.72

Note. Same as in Table 4.

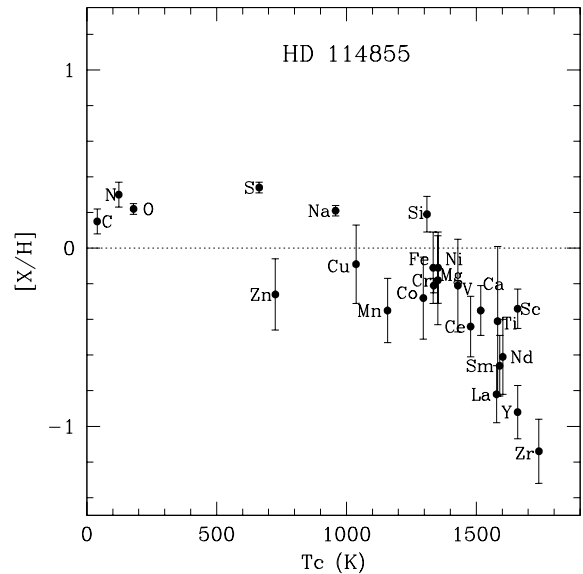


Figure 12. Abundance $[X/H]$ versus condensation temperature T_C for HD 114855.

Table 11. Elemental abundances for HD 114855

Species	$\log \epsilon_{\odot}$	[X/H]	s.d.	N	[X/Fe]
C I	8.39	+0.15	± 0.14	15	+0.26
N I	7.78	+0.30	± 0.17	3	+0.41
O I	8.66	+0.17	± 0.09	4	+0.28
Na I	6.17	+0.21	± 0.05	2	+0.32
Mg I	7.53	-0.21	± 0.06	4	-0.10
Si I	7.51	+0.19	± 0.10	21	+0.30
S I	7.14	+0.34	± 0.11	5	+0.45
Ca I	6.31	-0.35	± 0.11	8	-0.24
Sc II	3.05	-0.34	± 0.15	5	-0.23
Ti I	4.90	-0.32	± 0.19	3	-0.21
Ti II	4.90	-0.50	± 0.12	9	-0.39
V I	4.00	-0.18	± 0.11	3	-0.07
V II	4.00	-0.25	± 0.16	5	-0.14
Cr I	5.64	-0.29	± 0.10	10	-0.18
Cr II	5.64	-0.27	± 0.08	9	-0.16
Mn I	5.39	-0.35	± 0.08	9	-0.24
Fe I	7.45	-0.11	± 0.12	167	
Fe II	7.45	-0.11	± 0.13	25	
Co I	4.92	-0.16	± 0.17	5	-0.05
Co II	4.92	-0.21	± 0.15	2	-0.10
Ni I	6.23	-0.11	± 0.14	44	+0.00
Cu I	4.21	-0.09	± 0.21	2	+0.02
Zn I	4.60	-0.26	± 0.10	3	-0.15
Y II	2.21	-0.92	± 0.20	8	-0.81
Zr I	2.59	-1.14	± 0.24	5	-1.03
La II	1.13	-0.82	± 0.16	5	-0.71
Ce II	1.58	-0.44	± 0.16	6	-0.33
Nd II	1.45	-0.61	± 0.12	6	-0.50
Sm II	1.01	-0.66	± 0.14	6	-0.55

4.9 CNO abundances for HD 725

HD 725 (IRAS0091+5650) is a supergiant F5Ib-II star with mild Fe-deficiency and significant Na enhancement. A mild enrichment of light s-process elements have also been seen (Arellano Ferro, Giridhar & Mathias 2001). We have estimated abundances of C, N, O in the present work. The estimate [C/H] of -0.04 even after correction for non-LTE effect remains near solar. We estimate [N/H] of 0.72 which after accounting for non-LTE effect indicates [N/H] of $+0.4$. [O/H] is not much different from the solar value. The abundances are indicative of CN processing proton capture on ^{22}Ne occurring in Hydrogen burning region.

5 DISCUSSION

Our sample contains the objects HD 725, HD 842, HD 1457, HD 9233 and HD 61227 which show very moderate metal deficiency and have similar atmospheric parameters but they exhibit strong [N/C] anomalies (Table 12). The observed [N/C] ratios even after NLTE correction exceed the prediction of FDU by a varying degree. The evolutionary calculation of Schaller et al. (1992) predict [N/C] of $+0.6$ for stars in the mass range of $2\text{-}15 M_{\odot}$. Since A-F supergiant stars are likely to have B type main sequence progenitors, hence it is instructive to use $\Delta \log \text{N/C} = [\text{N/C}]_{*} - [\text{N/C}]_{B}$ to make comparison with evolutionary predictions. The published abundances of B stars have been reviewed by Venn (1995) who after applying suitable NLTE corrections found a mean [C/H] of -0.35 and [N/H] of -0.21 or $[\text{N/C}]_{B}$ of 0.14

Table 12. [N/C] anomalies in selected stars.

Star	[C/Fe] _{NLTE}	[N/C] _{NLTE}	[N/C] _{*-B}	[Na/Fe]
HD 725	-0.10	+0.82	+0.68	+0.51
HD 842	-0.30	+1.00	+0.86	+0.49
HD 1457	-0.20	+1.55	+1.41	+0.71
HD 9233	-0.04	+0.88	+0.74	+0.44
HD 61227	-0.25	+0.90	+0.76	+0.52

for main sequence B stars. The [N/C] ratio after the above mentioned correction remains higher than the FDU prediction. The observed CNO abundances do not agree with the predictions of HBB which require low carbon abundances. Further, we do not have other indications of post-AGB evolution such as photometric and radial velocity variations, variable emission components in hydrogen lines.

It is possible that this excess [N/C] is related to the rotational induced mixing on the main sequence. The evolutionary models including rotation have been generated by Maeder & Meynet (2000) for a range of stellar masses. Here the [N/C] enhancement is caused by partial mixing of CN cycled gas from the stellar interior due to main sequence rotation. Hence, in rotating models the N enrichment can occur even at the main sequence. The effect is enhanced at lower metallicities. Within a small range of $\log T_{\text{eff}}$ the [N/C] appears to be correlated with stellar mass.

Unfortunately, for our sample stars the distances are not known and hence the luminosity and the mass cannot be estimated. We can only make a qualitative study of the [N/C] trend exhibited by them. Although the observed $v \sin i$ ranges between 5 and 20 km s^{-1} , they cannot be used to infer the rotation velocity at the main sequence. Within these limitations and assuming the same rotation velocity at main sequence, it can be said that HD 1457 might have had the most massive progenitor and HD 9233 the least of this group. It is interesting to note a weak correlation between [N/C] and [Na/Fe] (Table 12), since [Na/Fe] is believed to be related to the mass of the progenitor (Sasselov 1986, Takeda & Takada Hidai 1994).

On the other hand, HD 53300, CpD $-62^{\circ}5428$, HD 105262, HD 114855, display several post-AGB characteristics as described in their respective sections. With the exception of HD 114855 all of them are significantly metal poor.

From the present sample of candidate stars only a modest fraction (four out of nine) turned out to be post-AGB objects. But these post-AGB stars have a large spread in temperature (6000K to 8500K) and they cannot be distinguished from other sample stars through their IR fluxes, Strömgren c_1 index or galactic latitudes. High resolution abundance analyses are necessary to identify post-AGB objects among the candidates.

6 SUMMARY AND CONCLUSIONS

Our present investigation of A-G superagints (with or without IR fluxes) has led to confirmation of post-AGB nature of candidates stars such as HD 105262, HD 53300 and CpD $-62^{\circ}5428$ and HD 114855. We find the signature of dust-gas separation process for HD 105262, HD 53300, CpD

-62°5428 and HD 114855, although the effect is mildest for HD 114855. For CpD -62°5428, the reduced scatter in [X/H] versus FIP plot indicates that the possibility of low FIP elements escaping as stellar wind cannot be ruled out. A time series photometric and spectroscopic monitoring is required to detect pulsation and shock seen in RV Tauri and related stars. Other stars exhibit over-abundances of N possibly caused by rotational induced mixing in addition to CN processing. The list of high Strömgren c_1 index by Bidelman (1993) of high galactic latitude stars contains many promising post-AGB candidates. The abundance data, in particular CNO, can help in identifying the promising objects over a range of atmospheric parameters which in turn will provide clues towards better understanding of various subgroups found in post-AGB stars.

ACKNOWLEDGMENTS

We are grateful to Dr. Jesús Hernández for taking the spectra of CpD -62°5428 and HD 114855 at Las Campanas Observatory and to Prof. David Lambert for providing us with the McDonald spectrum of HD 53300 and HD 105262. Valuable comments and suggestions from the referee, Prof. H. van Winckel are gratefully acknowledged. We are thankful to CONACyT Mexico and Dept of Science and Technology, India for the grant allotted under the exchange program DST/INT/Mexico/RP0-06/07 for supporting the visit by AAF to India. AAF also acknowledges support from the program PAPIIT-UNAM through grant IN114309-3. This work has made extensive use of SIMBAD database and the ADS to which we are thankful.

REFERENCES

Abt, H. A., Morrell, N. I., 1995, ApJS, 99, 135
 Arellano Ferro, A., Giridhar, S., Mathias, P., 2001, A&A, 368, 250
 Arellano Ferro, A., Giridhar, S., Rojo Arellano E., 2003, RMA&A, 39,3
 Bakker, E. J., Lambert, D. L., 1998, ApJ, 508, 387
 Baranne, A., Queloz, D., Mayor, M. et al., 1996, A&AS, 119, 373
 Beavers, W.I., Eitter, J.J., 1986, ApJS, 62, 147
 Bhatt, H.C., Manoj, P., 2000, A&A, 362, 978
 Bidelman, W.P., 1951, ApJ, 113,304
 Bidelman, W.P., 1993, in Luminous High-Latitude Stars, ASP Conf. Ser. 45, 47
 Biemont, E., Grevesse, N., Hannaford, P., Lowe, R. M., 1981, ApJ, 248, 867
 Blöcker, T., 1995, A&A, 299, 755
 Bond, H.E., Luck, R.E., 1987, ApJ, 312, 203
 Bravo-Alfaro, H., Arellano Ferro, A., Schuster, W. H., 1997, PASP, 109, 958
 Boothroyd, A. I., Sackmann, I.J., 1999, ApJ, 510, 232
 Boyarchuck, A.A., Lyubimkov, L.S., Sakhbullin N.A. 1985, Astrophysics, 22, 203
 Brown, J.A., Wallerstein, G., Oke, J.B., 1990, AJ, 100, 1561
 Bujarrabal, V., Castro-Carrizo, A., Alcolea, J., Neri, R., 2005, A&A, 441, 1031
 Castelli, F., Kurucz, R. L., 2003, in Modelling of Stellar Atmospheres, Poster Contributions. Proceedings of the 210th Symposium of the International Astronomical Union held at Uppsala University, Uppsala, Sweden, 17-21 June, 2002. Edited by N. Piskunov, W.W. Weiss, and D.F. Gray. Published on

behalf of the IAU by the Astronomical Society of the Pacific, p.A20
 Cayrel de Strobel, G., Hauck, B., Francois, P., Thevenin, F., Mermilliod, M., Bordes, S., 1992, A&AS, 95, 273
 Conlon, E.S., Dufton, P.L., McCausland, R.J.H., Keenan, F.P., 1993, ApJ, 408, 593
 Conlon, E.S., Dufton, P. L., R. J.H., Keenan, F. P., 1994, A&A, 290, 897
 Cortes, C., Silva, J.R.P., Recio-Blanco,A., Catelan, M., Anscimento, J.D., Medeiros, J.R., 2009, ApJ, 704, 750
 Davidson, M.D., Snoek, L.C., Volten, H., Donszelmann, A., 1992, A&A, 255, 457
 Deroo,P., van Winckel, H., 2007, BaltA, 16, 145
 Deroo, P., van Winckel, H., Min, M., Waters, L.B.F.M., Verhoelst, T., Jaffe, W., Morel, S., Paresce, F., Richichi, A., Stee, P., Wittkowski, M., 2006, A&A, 450, 181
 Duflot,M., Figon, P., Meyssonnier,N., 1995, A&AS, 114, 269
 Fokin, A.B., 1991, MNRAS, 250, 258
 Führ, J.R., Wiese, W.L., 2006, J. Phys., Ref., Data, 35, 1669
 Gallagher, A., 1967, Phys. Rev., 157, 24
 García-Lario,P. 1992, Ph.D. Thesis, U. La Laguana, Spain
 García-Lario, P., Perea Calderón, J.V., 2003 in *Exploiting the ISO data archive, Infrared astronomy in Internet Age*, ESA SP-511, 97
 García-Lario, P. 2006, in *Planetary Nebulae in our Galaxy and Beyond*, Proc. IAU symposium No 234, 63
 García-Lario, P., Manchado, A., Pych, W., Pottasch, S. R., 1997, A&AS, 126, 479
 Gielen, C., van Winckel, H., Matsuura, M., Min, M., Deroo, P., Waters, L. B. F. M., Dominik, C., 2009, A&A, 503, 843
 Giridhar, S., Arellano Ferro A., 2005, A&A, 443, 297
 Giridhar, S., Arellano Ferro, A., Parrao, L., 1997, PASP, 109, 1077
 Giridhar, S., Goswami, A., 2002, BASI, 30, 501
 Giridhar, S., Lambert, D. L., Reddy, B. E., Gonzalez, G., Yong, D., 2005, ApJ, 627, 432
 Giridhar, S., Lambert, D. L., Gonzalez, G., 2000, ApJ, 531, 521
 Giridhar, S., Kameswara Rao, N. K., Lambert, D. L., 1994 ApJ, 437, 476
 Glaspey, J.W., 1982, ApJL, 258, L71
 Gray, R. O., Napier, M. G., Winkler, L. I., 2001, AJ, 121, 2148
 Gray, R.O., Olsen, E. H., 1991, A&AS, 87, 541
 Gontcharov, G.A., 2006, Astron. Lett., 32, 759
 Gonzalez, G., Lambert, D.L., Giridhar, S., 1997, ApJ, 481, 452
 Gonzalez, G., Wallerstein, G., 1996, MNRAS, 280, 515
 Grenier, S., Baylac, M.-O., Rolland, L., Burnage, R., Arenou, F., et al.,1999, A&AS, 137, 451
 Gronewegen, M.A.T., de Jong, T., 1993, A&A, 267, 410
 Gronewegen, M.A.T., Marigo,P., 2004, in *Asymptotic Giant Branch stars*, Eds Habing,H.J. and Olofsson,H, Springer-Verlag, p105
 Hannaford, P., Lowe, R. M., Grevesse, N., Biemont, E., Whaling, W., 1982, ApJ, 261, 736
 Hartog, E.A., Lawler, J.E., Sneden, C., Cowan, J.J., 2003, ApJ, 148, 543
 Hauck, B., Mermilliod, M., 1998, A&AS, 129, 431
 Herwig, F., 2004, ApJS, 155, 651
 Herwig, F., 2005, ARA&A, 43, 435
 Hrivnak, B.C, Kwok, S. and Volk, K.M. 1989, ApJ 346,,265
 Iben,I., Renzini,A., 1983, ARA&A, 21, 271
 Kameswara Rao, N. K., Reddy, B. E., 2005, MNRAS 357, 255
 Kameswara Rao, N. K., Sriram, S., Jayakumar, K., Gabriel, F., 2005, JApA., 26, 331
 Karakas, A.I., Lattanzio, J.C., Pols, O.R., 2002, PASA, 19, 515
 Kazarovets, E. V., Samus, N. N., Durlevich, O. V., Frolov, M. S., Antipin, S. V., Kireeva, N. N.; Pastukhova, E. N., 1999, IBVS No. 4659, 1
 Klochkova, V.G., 1995, MNRAS, 272, 710

- Klochkova, V.G., Panchuk, V.E., 1987, *Astron. Zh.*, 64, 74
- Koen, C., Eyer, L., 2002, *MNRAS*, 331, 45
- Kovtyukh, V. V., 2007, *MNRAS*, 378, 617
- Kurucz, R.L., 1993, *ATLAS9 Stellar atmosphere programs and 2 km s⁻¹ grin CDRoM Vol. 13.* (Cambridge: Smithsonian Astrophysical Observatory)
- Kwok, S., Boreiko, R.T., Hrivnak, B.J., 1987, *ApJ*, 312, 303
- Kwok, S., Hrivnak, B.J., Geballe, T.R., 1990, *ApJ*, 360, L23
- Lattanzio, J.C., Frost, C., Cannon, R., Wood, P.R., 1996, *Mem. Soc. Astron. Italiana*, 67, 729
- Lambert, D. H., Hinkle, K. H., Luck, R. E., 1988, *ApJ*, 333, 917
- Lattanzio, J, Frost, C., Cannon, R., Wood P.R. 1996, *Mem Soc Atron Italiana*, 67, 729.
- Lawler, J.E., Sneden, C., Cowan, J.J., Evans, I.I., Den Hartog, E.A., 2009, *ApJ*, 182, 51
- Lawler, J.E., Hartog, E.A., Sneden, C., Cowan, J.J., 2006, *ApJ*, 162, 227
- Lawler, J.E., Bonvallet, G., Sneden, C., 2001a, *ApJ*, 556, 452
- Lawler, J.E., Wickliffe, M.E., Den Hartog, E.A., Sneden, C., 2001b, *ApJ*, 563, 1075
- Lébre, A., Gillet, D. 1992, *A&A*, 255, 221
- Lébre, A., Mauron, N., Gillet, D., Barthes, D., 1996, *A&A*, 310, 923
- Ljung, G., Nilsson, H., Asplund, M., Johansson, S., 2006, *A&A*, 456, 1181
- Lloyd Evans, T. 1990, *MNRAS*, 243, 336
- Lodders, K., 2003, *ApJ*, 591, 1220
- Luck, R.E., Bond, H.E., Lambert, D. L., 1990, *ApJ*, 357, 188
- Luck, R.E., Lambert, D.L., Bond, H. E., 1983, *PASP*, 98, 413
- Maas, T., van Winckel, H., Waelkens, C., 2002, *A&A*, 386, 504
- Maas, T., Giridhar,S., Lambert, D.L., 2007, *ApJ*, 463, 243
- Martin, J.C. 2004, *AJ*, 128, 2474
- McCausland, R.J.H., Conlon, E.S., Dufton, P.L., Keenan, F.P., 1992, *ApJ*, 394, 298
- Meléndez, J., Barbuy, B., 2009, *A&A*, 497, 611
- de Medeiros, J.R., Udry,S., Burki, G., Mayor, M. 2002, *A&A*, 395,97
- Moehler, S., Heber, U., 1998, *A&A*, 335, 985
- Moehler, S., Heber, U., Lemke, M., Napiwotzki, R., 1998, *A&A*, 339, 537
- Napiwotzki,R., Schönberner, D., Wenske,V. 1993, *A&A*, 268, 653
- Olsen, E.H., 1983, *A&AS*, 54, 55
- Ortiz R., Lorenz-Martins S., Maciel W.J., Rangel E.M., 2005, *A&A*, 431, 565
- Oudmaijer, R.D., Bakker, E.J. 1994, *MNRAS*, 271, 615
- Oudmaijer, R.D., Waters, L. B. F. M., van der Veen, W. E. C. J., Geballe, T. R., 1995, *A&A*, 299, 690
- Oudmaijer, R.D., van der Veen, W.E.C.J., Waters, L.B.F.M., Trams, N.R., Waelkens, C., Engelsman, E., 1992, *A&AS*, 96, 625
- Oudmaijer, R.D., Waters, L. B. F. M, van der Veen, W. E. C. J., Geballe, T.R. 1995, *A&A*, 299, 690
- Parthasarathy, M., Reddy, B. E., 1993, *Bull. ASI*, 21, 609
- Pottasch, S. R., Parthasarathy, M., 1988, *A&A*, 192,182
- Preston, G.W., Sneden, C., 2000, *AJ*, 120, 1014
- Reddy, B.E., Lambert, D. L., Allende Prieto, C., 2006, *MNRAS*, 367, 1329
- Reddy, B.E., Lambert, D. L., Gonzalez, G., Yong, D., 2002, *ApJ*, 564, 482
- Reddy, B.E., Parathasarathy, M., Sivarani, T., 1996, *A&A*, 313, 191
- Reyniers, M., 2002, PhD Thesis, Katholieke Universiteit Leuven, Belgium
- Royer F., Grenier S., Baylac M.-O., Gomez A.E., Zorec J., 2002, *A&A*, 393, 897
- de Ruyter, S., van Winckel, H., Maas, T., Lloyd Evans, T., Waters, L.B.F.M., Dejonghe, H., 2006, *A&A*, 448, 641
- Sasselov, D.D., 1986, *PASP*, 98, 561
- Szczerba, R., Siódmiak, N., Stasińska, G., Borkowski, J., 2007, *A&A*, 469, 799
- Schaller, G., Schaerer, D., Mainer, G., Maeder, A., 1992., *A&AS*, 96, 269
- Schiller, F., Przybilla, N., 2008, *A&A*, 479, 849
- Schmidt- Kaler, Th., 1982, in *Numerical Data and Functional Relationships in Science and Technology*, ed. K. Schaifers & H.H. Vogt (Springer-Verlag)
- Sneden, C., Lawler, J.E., Cowan, J.J., Evans, I.I., Den Hartog, E.A., 2009, *ApJS*, 182, 80
- Sobeck, J. S., Lawler, J. E., Sneden, Ch., 2007, *ApJ*, 667, 1267
- Suárez, O., Garca-Lario, P., Manchado, A., Manteiga, M., Ulla, A., Pottasch, S. R., 2006, *A&A*, 458, 173
- Szczerba, R., Siódmiak, N., Stasinska, G., Borkowski, J., 2007, *A&A*, 469, 799
- Takeda, Y., Takada-Hidai, M., 1994, *PASJ*, 46, 395
- Takeda, Y., Takada-Hidai, M., 1998, *PASJ*, 50, 629
- Thévenin, F., Idiart, T.P., 1999, *ApJ*, 521, 75
- Tull, R.G., Macqueen, P.J., Sneden, C., Lambert, D.L., 1995, *PASP*, 107, 251
- Van de Steene, G.C., van Hoof, P.A.M., Wood, P.R., 2000, *A&A*, 362, 984
- Van de Steene, G.C., Pottasch, S.R., 1993, *A&A*, 274, 895
- van der Veen, W.E.C.J., Habing, H.J., 1988, *A&A* 194, 125
- van der Veen, W.E.C.J., Habing, H.J., Geballe, T.R., 1989 *A&A*, 226, 108
- van Winckel, H., 2003, *Ann. Rev. A&A*, 41, 391
- van Winckel, H., Waelkens, C., 1995, *Ap&SS*, 224, 581
- van Winckel, H., Waelkens, C. and Waters, LBFM, 1995, *A&A*, 293, L25
- van Winckel, H. 1997, *A&A*, 319, 561
- van Winckel, H., Waelkens, C., Waters, LBFM, Molster,F.J.,Udry,S. and Bakker, E.J., 1998, *A &A*, 336, 17
- Venn, K.A., 1995, *ApJ* 449, 839
- Walker, H.J., Wolstencroft, R.D., 1988, *PASP*, 100, 1509
- Waters, L.B.F M, Cami, J., de Jong, T., Molster, F. J., van Loon, J.Th., Bouwman, J., et al., 1998, *Nature*, 391, 868
- Waelkens, C., van Winckel, H., Bogaert, E., Trams, N. R., 1991, *A&A*, 251, 495